筑波大学

University of Tsukuba

博士（人間生物学）学位論文

Ph.D. Dissertation in Human Biology

Glucocorticoids Impair the Tissue Regenerative Function of Mesenchymal Stem Cells

(ステロイド治療は間葉系幹細胞の組織修復能を低下させる)

2017

筑波大学グローバル教育院

School of Integrative and Global Majors in University of Tsukuba

Ph. D. Program in Human Biology

Toshiki Kato

Table of Contents

Chapter I: General Over View

1.1. Background

Glucocorticoids are popular anti-inflammatory drug, on the other hand, the strong immunomodulatory effect causes undesirable effects including osteonecrosis of the femoral head (ONFH). Mesenchymal stem cells (MSCs) are considered as promising cells to treat ONFH due to their multi-differentiation potential and the ability to produce cytokines that recruit various types of cells for tissue regeneration. However, the effect of glucocorticoid therapy on MSCs has not been fully elucidated yet. The present study aimed to investigate the effect of glucocorticoids on the function of bone regeneration in MSCs. Moreover, I aimed to characterize the function of MSCs derived from steroid-induced ONFH patients who received high-dose and long-period glucocorticoid therapy and elucidated the underlying molecular mechanism.

1.2. Results

1) BM-MSCs derived from steroidal ONFH patients have less proliferative and self-renewal ability compared with BM-MSCs derived from traumatic ONFH patients

To clarify the effect of glucocorticoid on the character of bone marrow-derived MSCs (BM-MSCs), colony formation assay using primary bone marrow aspirate from traumatic or steroid-induced ONFH patients was performed, and I found

bone marrow derived from steroid-induced ONFH patients contained less number of BM-MSCs than traumatic ONFH patients. In addition, BM-MSCs derived from steroid-induced ONFH patients (sBM-MSCs) showed less and unstable proliferative ability compared with BM-MSCs derived from traumatic ONFH patients.

2) The osteogenic potential of AT-MSCs derived from steroidal ONFH patients are impaired by inhibition of wnt/β-catenin signaling

In order to investigate the differences in the characteristics between bone marrow and adipose tissue, I next isolated and analyzed adipose tissue derived MSCs from steroid-induced ONFH patients (sAT-MSC). Their proliferative potential was not impaired; however, the osteogenic potential of sAT-MSCs was decreased compared with AT-MSCs derived from traumatic ONFH patients (nAT-MSC). Therefore, I investigated the expression of osteogenic genes and alkaline phosphatase (ALP), which regulated the calcification of extracellular matrix, was downregulated in sAT-MSCs during osteogenesis. To confirm whether ALP is responsible for the impairment of osteogenesis in sAT-MSCs, ALP-overexpressing sAT-MSCs were established and overexpression of ALP recovered the impaired osteogenic ability in sAT-MSCs.

To identify the downregulation mechanism of ALP in sAT-MSCs, I focused on wnt/β-catenin signaling that plays an important role in bone development. I found that Dickkopf1 (Dkk-1), one of the known antagonists of

wnt/βcatenin signaling, was upregulated in sAT-MSCs, where, in this situation, the impaired osteogenic potential was rescued when Dkk-1 shRNA (shDkk-1) was transfected. Consistent with these results, nAT-MSCs chronically exposed to dexamethasone in vitro, which mimicked the microenvironment of sAT-MSCs, also showed reduced osteogenic differentiation ability and increased expression of Dkk-1 that downregulated ALP.

3) Lowered bone regeneration capacity of sAT-MSCs is reversed by shDkk1

The abnormal expression of osteogenesis-related factors in sAT-MSCs suggested that sAT-MSCs might have less bone regenerative capacity than nAT- MSCs, possibly because of the overexpression of Dkk-1. Therefore, I examined the bone regenerative capacity of nAT-MSCs, sAT-MSCs, nAT-MSCs transfected with mock, sAT-MSCs transfected with mock, and sAT-MSCs transfected with shDkk-1, using the critical-sized calvarial defect mouse model. nAT-MSCs and mock-transfected nAT-MSCs could facilitate bone formation, whereas sAT-MSCs showed impaired bone regenerative capacity. In contrast, shDkk-1-transfected sAT-MSCs showed significant increases in bone regenerative capacity compared with the sAT-MSCs transfected with mock. To prove the presence of transplanted AT-MSCs in the repaired bone regions, I performed immunohistological analysis using anti-human osteipontin (hOPN) antibody, which is a maker of mature osteoblast, and found there were hOPN-positive cells in the repaired bone region with nAT-MSCs,

mock-transfected nAT-MSCs and shDkk-1-transfected sAT-MSCs. On the other hand, no positive cells were observed in sAT-MSCs and mock-transfected sAT-MSCs at the transplanted regions. Of note, plasma Dkk-1 levels were elevated in steroid-induced ONFH patients.

1.3. Discussion

In the present study, I demonstrated that chronic glucocorticoid treatment impaired the proliferative potential of BM-MSCs whereas proliferation in AT-MSCs derived from steroid-induced ONFH was not affected. On the other hand, the osteogenic ability of sAT-MSCs was impaired through the downregulation of wnt/β-catenin signaling due to highly expressed Dkk-1. Interestingly, the elevated level of Dkk-1 was also observed in the plasma from steroid-induced ONFH patients. These results suggested Dkk-1 expression would be the key promoter of AT-MSCs as a useful therapy source.

1.4. List of abbreviations

ALP	Alkaline phosphatase
AT-MSC	Adipose tissue derived mesenchymal stem cells
bFGF	Basic fibroblast growth factor
BM-MSC	Bone marrow derived mesenchymal stem cell
BMP-2	Bone morphogenetic protein 2
CD	Cluster of Differentiation
CFU-F	Colony-forming unit-fibroblasts
Dex	Dexamethasone
Dkk-1	Dickkopf-1
EGF	Epidermal Growth Factor
ELISA	Enzyme-Linked ImmunoSorbent Assay
FBS	Fetal Bovine Serum
IMDM	Iscove's Modified Dulbecco's Media
MSC	Mesenchymal Stem Cell
ONFH	Osteonecrosis of the femoral head
PBS	Phosphate Buffered Saline
Runx2	Runt-related transcription factor 2
µCT	Micro computed-tomography

Chapter II: Elevated expression of Dkk-1 by glucocorticoid treatment impairs bone regenerative capacity of adipose tissue-derived mesenchymal stem cells

2.1. Introduction

2.1.1. Mesenchymal stem cells

Mesenchymal stem cells (MSCs) are one of the tissue stem cells and possess multipotent, self-renewing capacity, and divergent differentiation capacity (Dominici et al., 2006; Uccelli, Moretta, & Pistoia, 2008). Originally, MSCs were identified as stromal colony forming cells (CFU-F) in bone marrow (Friedenstein, Chailakhjan, & Lalykina, 1970). Although the physiological function of endogenous MSCs have not been elucidated, it is known that MSCs surround blood vessels in mesenchymal tissue and considered to be contributed to maintain microenvironment by their differentiation ability and cytokine production. Until now, it has been reported that MSCs can be isolated from bone marrow, umbilical cord blood, placenta, adipose tissue, dental pulp, and endometrium tissue (Uccelli et al., 2008). International Society of Cell Therapy (ISCT) defined the minimal criteria of MSCs as follow; 1) adherence to plastic, 2) specific surface antigen expression, ≧95% of the MSC population must express CD105, CD73 and CD90,and lack expression (≦2% positive) of CD45, CD34, CD14 or CD11b, CD79a or CD19 and HLA class II, 3) differentiation capacity into osteoblast, adipocyte and chondrocyte under differentiating condition (Dominici

et al., 2006).

Therefore, MSCs are currently the most promising cells for several kinds of regeneration and tissue engineering. These facts attract high attention to MSCs use as cell therapies for several kinds of diseases. Our laboratory and other groups have reported that disease-oriented MSCs differ in key MSC characteristics dependent on both disease-related conditions as well as medication side effects (Khanh et al., 2017; Serena et al., 2016; Trinh et al., 2016; Yamanaka et al., 2014).

2.1.2 Clinical usage of glucocorticoid

Glucocorticoids, a drug class analogous to endogenous steroid hormones, are an important anti-inflammatory drug which has been used for their strong immunomodulatory effects (Schleimer, 1993). Therefore, they are widely used to treat a broad range of indications (Schleimer, 1993). However, despite their benefits, glucocorticoids cause several complications, such as diabetes, hypertension, delayed wound healing, and osteoporosis (Barnes, 1998; Schäcke, Döcke, & Asadullah, 2002). Both beneficial and side effects are known to be mediated via the glucocorticoid receptor (GR) which is expressed in most cell types (Barnes, 1998; Schäcke et al., 2002). Glucocorticoids bind to GR and translocate into a nucleus to regulate target genes that have glucocorticoid responsive element on DNA. In addition, glucocorticoid also affects the regulation of other glucocorticoid responsive genes involves interactions

between glucocorticoid/GR complex and other transcription factor including nuclear factor-kB (NF-kB). These signals inhibit inflammation and other biological events, that induce both beneficial and side effects (Rhen & Cidlowski, 2005).

2.1.3. Side effects of glucocorticoid on bone tissue

Among these side effects, impairment of bone tissues, such as osteoporosis, is considered as the most common complication (Cooper & Hardy, 2011). Osteoporosis is a catabolic bone disease which manifests as a decrease in both bone mass and density as well as degradation of bone microstructure which makes the bone fragile (Lukert & Raisz, 1990). Glucocorticoids induce osteoporosis by impairment of calcium absorption and increased calcium excretion in kidneys (Lukert & Raisz, 1990). In bone tissue, osteoblasts are directly affected and their proliferation and maturation are impaired by glucocorticoids (Clevers, 2006; Lukert & Raisz, 1990). In addition, suppression of osteoblast function is reported to be associated with changes in wnt/β-catenin signaling, an important signal for bone remodeling and development (Ohnaka, Taniguchi, Kawate, Nawata, & Takayanagi, 2004). Previous studies demonstrated that glucocorticoids unregulated antagonists for wnt/β-catenin signaling, including Dickkopf1 (Dkk-1) and secreted frizzled-related protein-1 (sFRP-1), in osteoblasts (Hayashi et al., 2009; Ohnaka et al., 2004). Importantly, in addition to osteoporosis, long-term and high-dose glucocorticoid therapy is

also known as the major risk factor for steroid-induced osteonecrosis of the femoral head (ONFH) (FISHER & BICKEL, 1971; Weinstein, 2012), a bone tissue ischemia involving death of osteocytes (Jones & Hungerford, 2004; Urbaniak, Coogan, Gunneson, & Nunley, 1995).

2.1.4. Glucocorticoids affect osteogenesis *in vitro*

Glucocorticoids are also known to support osteogenic differentiation of MSCs *in vitro* (Cheng, Yang, Rifas, Zhang, & Avioli, 1994; Mostafa et al., 2012; Tran et al., 2011). On the other hand, it has been reported that glucocorticoids suppress the osteogenic differentiation of a murine osteoblast cell line, MC3T3-E1 (Hayashi et al., 2009). Previous studies reported that excessive amounts of glucocorticoids cause MSCs to favor to the adipocyte lineage rather than bone or muscle lineages (Cooper & Hardy, 2011; Yao, Cheng, Pham, et al., 2008). However, very few studies have focused on the influences of long-term and high-dose glucocorticoid treatments on the characteristics and differentiation ability of patient-derived MSCs. This raises questions as to how excessive glucocorticoids affect MSCs differentiation ability; however, the influences of long-term and high-dose glucocorticoid treatment on endogenous MSCs have not been elucidated. Moreover, studies on the characteristics and the therapeutic function of MSCs derived from steroid-induced ONFH patients have not been well focused.

In this study, I aimed to clarify the mechanism of how glucocorticoids impair the differentiation of MSCs into osteoblasts to determine the possibility of using glucocorticoid treated-MSCs for clinical use of bone fractures or bone-related diseases. I investigated the general characteristics of bone marrow (BM-) and AT-MSCs derived from ONFH patients undergoing high-dose treatment with glucocorticoids.

2.2. Materials and Methods

2.2.1. Isolation and culture of bone marrow and adipose tissue-derived mesenchymal stem cells

All human cell experiments were approved by the Ethic committee of the University of Tsukuba. Human bone marrow and adipose tissues from steroid-induced ONFH patients (bone marrow: n=13, maximum dose of glucocorticoid=46.5 ± 12.1 mg , current dose of glucocorticoid= 7.96 ± 6.42 mg, age=40.5±10.0; adipose tissue: n=6, maximum dose of glucocorticoid=70.0 ± 29.5 mg, current dose of glucocorticoid=8.58 ± 2.25 mg, male=2, female=4, age=41.5 ± 11.2) and traumatic ONFH patients (bone marrow: n=5, no systemic glucocorticoids administration, age=47.5 ± 9.9; adipose tissue: n=6, no systemic glucocorticoids administration, male=2, female=4 , age=60.5 ± 20.4) were obtained from the Department of orthopedic surgery, University of Tsukuba Hospital (Tsukuba, Japan).

Adipose tissue-derived mesenchymal stem cells (AT-MSCs) were isolated as previously described (Sato et al., 2015). Briefly, human adipose tissue was minced with scissors and treated with 0.1% collagenase (Nitta Gelatin, Osaka, Japan) in PBS, 20% FBS (Hyclon, UT, USA) for 45 min at 37°C. After incubation, samples were centrifuged and cultured in maintenance medium [Iscove's modified Dulbecco medium (Invitrogen, CA, USA) /10% FBS/ 5 ng/mL bFGF (PeproTech, London, UK), and 0.1% (v/v) penicillin-streptomycin (100 U/mL penicillin, 0.1 mg/mL streptomycin; Invitrogen)].

Bone marrow-derived mesenchymal stem cells (BM-MSCs) were isolated as previously described (Kimura et al., 2013). Briefly, BM-derived cells were put on a density gradient buffer (Histopaque 1.083 g/cm^3; Sigma-Aldrich, MO, USA) and centrifuged at 2000 rpm for 20 min at room temperature. Cells were harvested from middle layer and then cultured by the same method as used for AT-MSCs described above.

2.2.2. Colony forming unit of fibroblast assay (CFU-F)

For primary bone marrow aspirate, 2 ml bone marrow with acid citrate dextrose solution was diluted 5 times and seeded at 500 μl/well in 6-well plates (SUMILON, Tokyo, Japan) in maintenance medium. For cultured BM-MSCs, BM-MSCs were seeded at 100 cells / well in 6-well plates (SUMILON) in maintenance medium at P1. After 2 weeks, both primary bone marrow and BM-MSCs were fixed and stained with 0.5% crystal violet. Visible colonies were scored by macroscopic observation.

2.2.3. Long-term glucocorticoid exposure in vitro

For long-term glucocorticoid exposure assay, isolated cells from adipose tissue were directly cultured in maintenance medium with 100 nM, 10 nM, or 1 nM of dexamethasone (Sigma-Aldrich). AT-MSCs were seeded at 4×10^3 cells/cm^2 in T25 flask (SUMILON). After 5 passages, dexamethasone exposed cells were used for further experiments.

2.2.4. In vitro differentiation assay

AT-MSCs were evaluated for their differentiation ability into osteocytes, adipocyte, and chondrocyte. AT-MSCs were seeded in 4-well IVF plates (BD Falcon BD Falcon, MA, USA) at passages 5 to 8. Adipogenic differentiation was initiated by incubating in adipogenic differentiation medium [IMDM (Invitrogen) + 10% FBS, 0.5 mM 3-isobutyl 1-methylxantine (Sigma-Aldrich), 10 μg/ mL insulin (Wako), 0.1 mM dexamethasone (Sigma-Aldrich), and 200 μM indomethacin (Sigma-Aldrich)] as described previously (Tran et al., 2011), and the adipogenic ability was examined by Oil Red O staining (Muto Pure Chemicals, Tokyo, Japan). For the quantitation of adipogenic differentiation, Oil Red O was dissolved in isopropanol containing 2% IGEPAL (Sigma-Aldrich) solution and quantified by spectrometry at 492 nm.

Osteogenic differentiation was induced by incubation of cells in osteogenic differentiation medium [IMDM with 1% FBS, 10 mM β-glycerol (Sigma-Aldrich), 200 μM ascorbic acid (Sigma-Aldrich), 0.1 mM dexamethasone (Sigma-Aldrich), and 20 ng/mL EGF (PeproTech)] as described previously (Sato et al., 2015). Osteogenic differentiation was examined using 1% Alizarin Red S (Wako, Osaka, Japan) solution and alkaline phosphatase staining solution (Sigma-Aldrich). For the quantification of osteogenic differentiation, Alizarin red S was dissolved in Plank-Rychlo (Kanto-Kagaku, Tokyo, Japan) and analyzed by spectrometry at 480 nm. Alkaline phosphatase activity was examined

histologically with a Leukocyte Alkaline Phosphatase Kit (Sigma-Aldrich) according to the manufacturer's instructions.

Chondrogenic differentiation was performed by aggregate culture methods. 2.5×10^5 cells were seeded in low-cell adhesion 96-well plates (SUMILON) using chondrocyte differentiation medium [IMDM+1% FBS, 1% ITS-premix (BD Bioscience), 4 mM proline (Sigma-Aldrich), 50 μg/mL ascorbic acid, 0.1 mM dexamethasone, 1 mM sodium pyruvate (Sigma-Aldrich), 10 ng/mL TGF-β1 (PeproTech), and 20 ng/mL BMP-2 (PeproTech)] as described previously (Nagano et al., 2010). The spheroids were fixed and embedded in OCT compounds (Sakura Finetek, Tokyo, Japan). Frozen sections were cut to 7mm thickness and stained with toluidine blue and hematoxylin/eosin (Muto Pure Chemicals). To quantify differentiation, proteoglycans were measured by use of a mucopolysaccharide assay kit (Cosmo Bio, Tokyo, Japan). The assay was performed according to the manufacturer's instructions.

2.2.5. Analysis of immune phenotype

AT-MSCs were harvested and suspended in PBS containing 2% FBS and incubated with anti-CD13 (1:200), anti-CD14 (1:40), anti-CD31 (1:40), anti-CD34 (1:200), anti-CD45 (1:200), anti-CD73 (1:200), anti-CD90 (1:40), anti-CD105 (1:200), anti-CD166 (1:40), anti-HLA-ABC (1:200), and anti-HLA-DR (1:200) antibodies (BD Pharmingen, CA, Japan) at 4°C for 30 min. After incubation, the stained cells were washed and 15,000 cells at a time were analyzed using a

Gallios flow cytometer (Beckman Coulter, CA, USA). The data was processed with the help of FlowJo software (Tree Star, Ashland, OR). A positive expression profile was defined as a level of fluorescence greater than 99% of the corresponding isotype control-stained sample.

2.2.6. Gene expression analysis

Total RNA was isolated from cells using extraction reagent (Sepasol-RNA I Super G; Nacalai Tesque, Kyoto, Japan) and reverse transcription was performed with 1 μg of the total RNA using an RT-polymerase chain reaction kit (Toyobo, Osaka, Japan), following the manufacturer's instructions. The expression levels of target genes were analyzed using a 7500 Fast Real-Time PCR machine (Applied Biosystems, CA, USA) with Thunderbird SYBR qPCR Mix (Toyobo). Experiments were carried out in triplicate and data were calculated using the $2^{-\Delta\Delta CT}$ method. Data were normalized to β-actin mRNA. The sequences of the primers used for quantitative RT-PCR are shown in Table 1.

2.2.7. Alkaline phosphatase overexpression with retroviral constructs

Prepared AT-MSCs were infected using cell-free retroviral supernatant from PT67 cells producing MSCV–human ALP–IRES–EGFP or MSCV-IRES-EGFP for 8 hours with 4 μg/mL polybrene (Sigma-Aldrich). After 8 hours, the medium was changed to fresh medium and cells were expanded. Subsequently, GFP-positive cells were sorted by a Moflo XDP (Beckman Coulter) and

expanded for further experiments. The expression of human ALP mRNA was confirmed by qPCR.

2.2.8. Establishment of shDkk-1 AT-MSCs

OmicsLink shRNA Expression clone targeted Dkk-1 and scrambled control gene (GeneCopoeia, MD, USA) were transfected into HEK293T cells using the Lenti-Pac HIV Expression Packaging Kit (GeneCopoeia) and pseudo-viral particles were harvested. These particles were then transduced into target cells and selected with 4 μg/ml puromycin. The effect of shRNA of Dkk-1 was assessed by qPCR analysis.

2.2.9. Western blot

Cells were harvested and homogenized in RIPA buffer at 4 °C. Twenty micrograms of whole cell extracts in each well were electrophoretically separated on SDS-polyacrylamide gel and then electrotransferred to polyvinylidene difluoride membranes (Merck Millipore, MA, USA). The membranes were immunoblotted with primary antibody (anti-beta-catenin antibody: 1:2000, sc-7199, Santa Cruz Biotechnology, TX, USA; anti-actin antibody: 1:2000, sc-1616, Santa Cruz Biotechnology; anti-Dkk-1: 1:1000, AF1096, R&D, MN, USA). After extensive washing, the membranes were incubated with HRP-conjugated secondary antibodies (Vector Laboratories, CA, USA), and positive signals were analyzed by a luminescence imager (Image

Quant LAS4000; GE Healthcare, NY, USA) using chemiluminescence reagents (Merck Millipore). Data were normalized to β-actin protein level.

2.2.10. Enzyme-Linked Immuno Sorbent Assay (ELISA)

Human bone marrow was aspirated from anterior iliac crests for concentrated autologous bone marrow aspirate transplantation (CABMAT) therapy for ONFH patients (Yoshioka et al., 2011). The Dkk-1 (DuoSet ELISA Development Kit; R&D) level in aliquots of serum was measured using respective kits according to the manufacturer's instructions. Results were calculated by interpolation from a standard curve obtained using a series of recombinant human Dkk-1 concentrations.

2.2.11. Critical-sized calvarial defect model

All animal experiments were carried out under accepted principles of laboratory animal care (Approval number: 17-085, Guide for the Care and Use of Laboratory Animals, University of Tsukuba) and were approved by the Institutional Animal Care and Use Committee of the University of Tsukuba. BALB/c nu/nu mice (8 week old) (Oriental Yeast, Tokyo, Japan) were used as recipients. The critical-sized calvarial defect model was generated as described previously (Kajiyama et al., 2015). Briefly, mice were anesthetized using tribromoethanol (125 mg/kg; Wako) and non-healing critical-sized (4 mm) calvarial defects were created in the parietal bone of adult BALB/c nu/nu mice

using a biopsy punch (Kai Industries, Tokyo, Japan). Importantly, the dura mater was left undisturbed. Then, 1×10^6 AT-MSCs were transplanted with a collagen scaffold (Atelocollagen sponge Mighty®, KOKEN, Tokyo, Japan) into defects. The mice were divided into six groups: PBS (scaffold with PBS, N=5), nAT-MSC (N=5), sAT-MSC (N=5), nAT-MSC transfected with mock (N=5), sAT-MSC transfected with mock (N=5), and sAT-MSC transfected with shDkk-1 (N=5). The calcified defect area was assessed by microcomputed tomography (μCT) using the Aloka Latheta LCT-100 system (Hitachi, Tokyo, Japan).

2.2.12. Histological Analysis

Mice were sacrificed 3 months after transplantation of MSCs and skulls were dissected. For H & E staining, the skulls were fixed and decalcified. The fixed tissues were embedded in paraffin, and 5 μm serial sections were prepared. The sections were stained with hematoxylin/eosin solution (Muto Pure Chemicals). To assess whether transplanted MSCs contribute to the bone regeneration, immunohistological staining with anti-human osteopontin antibody (1:200, AF1433, R&D) was performed. All staining was observed under a BZ-X700 microscope (Keyence, Osaka, Japan).

2.2.13. Statistical analysis

Data were presented as mean±standard deviation (SD). The comparison of between two groups was analyzed by student's *t*-test. Tukey-Kramer test was

used to analyze the differences between more than three groups after one-way ANOVA analysis. Statistical analysis was performed using GraphPad Prism 5 software (CA, USA). Statistical significance was taken as $P<0.05$.

2.3. Results

2.3.1. Chronic glucocorticoid treatment impairs the number of MSCs in bone marrow and their proliferation potential *in vitro*

In order to analyze how long-term glucocorticoid treatment affects BM-MSCs characteristics, colony formation assays using primary BM aspirates from both traumatic (a cell source for normal BM-MSCs) or steroid-induced ONFH patients were performed. It has been reported that the MSC pool in the proximal femur of steroid-induced ONFH patients decreased while the function of their BM-MSCs was impaired (P Hernigou, Beaujean, & Lambotte, 1999; Wang et al., 2008). Consistent with the results, I found that steroid-induced ONFH patients had less CFU-F than traumatic ONFH patients (Steroid: 48.1 ± 48.6 vs Traumatic: 91.3 ± 54.9, Steroid: n=36, Traumatic: n=12, *$P < 0.05$) (Fig. 1A). I next examined self-renewal activity of BM-MSCs-derived from steroid-induced ONFH patients (sBM-MSCs) and normal BM-MSCs-derived from traumatic ONFH patients (nBM-MSCs). I found that sBM-MSCs showed less self-renewal activity than nBM-MSCs (sBM-MSC:7.6 ± 4.3 vs nBM-MSC:15.1 ± 2.8, n=5, *$P<0.05$) (Fig. 1B). Cell growth assays showed sBM-MSCs had lesser and more unstable proliferative activity compared with nBM-MSCs (Fig. 1C, D). Indeed, over half of sBM-MSCs could not be passaged more than 4 times. These results suggest that cell therapy using sBM-MSCs are contraindicated for clinical applications as they lose their proliferative capacity.

2.3.2. Steroid-induced ONFH patients derived AT-MSCs show less osteogenic differentiation potential

In order to investigate the differences in characteristics between MSCs derived from BM and adipose tissue (AT), I next isolated and analyzed AT-MSCs derived from steroid-induced ONFH patients. I found these AT-MSCs possess a higher and more stable proliferative activity than BM-MSCs (Fig. 1), suggesting that AT-MSCs would be an alternative useful source for future clinical applications. However, the effect of steroids on AT-MSCs is still unknown (Wyles et al., 2015). To determine this, AT-MSCs-derived from steroid-induced ONFH patients who received high dose glucocorticoid therapy (current dose: >5 mg /day, period: >2 years)(sAT-MSCs) were characterized and compared with the AT-MSCs-derived from traumatic ONFH patients (nAT-MSCs). Both sAT-MSCs and nAT-MSCs showed a fibroblastic morphology (Fig. 2A) and there was no significant difference in the proliferative activity between nAT-MSCs (doubling time: 43.3 ± 7.14 h) and sAT-MSCs (doubling time: 40.7 ± 8.07 h) (Fig. 2B, C). Furthermore, I analyzed the immune phenotype of nAT-MSCs and sAT-MSCs and found both AT-MSCs showed MSC-like immune phenotypes ($CD13^+$, $CD73^+$, $CD90^+$, $CD105^+$, $CD166^+$, HLA-ABC^+, $CD14^-$, $CD31^-$, $CD34^-$, $CD45^-$, and HLA-DR^-) (Fig. 2D).

I next examined the osteogenic differentiation ability of nAT-MSCs and sAT-MSCs at day 14 and 21 and found that both nAT-MSCs and sAT-MSCs

could differentiate into osteoblasts. However, sAT-MSCs showed a lower differentiation ability than nAT-MSCs (Day14: 0.089-fold; Day21: 0.43-fold vs nAT-MSCs) (Fig. 3A, B). In addition, the chondrogenic differentiation ability of sAT-MSCs was also reduced compared with nAT-MSCs. Adipogenic differentiation ability was also examined and no significant differences in adipogenesis were observed in both nAT-MSCs and sAT-MSCs (Fig. 3C-F).

To clarify the molecular mechanism of how osteogenic differentiation is impaired in sAT-MSCs, I analyzed the expression of osteogenic related genes at day 0, 7, and 14 after differentiation. Consistent with the results of Alizarin Red S staining, gene expression of bone alkaline phosphatase (ALP) was decreased in sAT-MSCs (Day 0: 0.049-fold, Day 7: 0.088-fold, Day14: 0.23-fold decrease vs nAT-MSC) (Fig. 4A). On the contrary, no significant changes in the expression of other osteogenic related genes, such as Runx2, osteocalcin, and osteopontin, were observed.

I next evaluated the ALP enzymatic activity in differentiated cells by alkaline phosphatase staining and found that sAT-MSCs showed reduced ALP activity on day 14 post-differentiation (Fig. 4B). To confirm whether ALP is responsible for the impairment of osteogenesis in sAT-MSCs, ALP-overexpressing sAT-MSCs were established by a retroviral infection and infected cells were confirmed by RT-PCR (Fig. 4C). After 14 days of differentiation, the calcium component was detected in the ALP-overexpressing sAT-MSCs as similar level as nAT-MSCs, whereas no improvement of

calcification was observed in mock-transfected sAT-MSCs (Fig. 4D). This data shows that overexpression of ALP may rescue the osteogenic differentiation ability of sAT-MSCs.

Several studies have reported that MSCs contribute to tissue repair due to their potential to produce many cytokines and chemokines instead of their differentiated cells (21). From this perspective, I assessed the expression of secretion factors promoting bone regeneration, such as BMP-2, in sAT-MSCs, and found that BMP-2 was downregulated in sAT-MSCs (Fig. 4E).

AT-MSCs derived from steroid-induced ONFH patients who received chronic glucocorticoid therapy had no differences in cell morphology, proliferation ability, immune phenotype, and adipogenic capacities compared to the nAT-MSCs. On the other hand, the osteogenic and chondrogenic ability of sAT-MSCs were significantly downregulated compared to nAT-MSCs. Of note, overexpression of ALP in sAT-MSCs rescued osteogenic differentiation ability, suggesting that sAT-MSCs possess osteogenic differentiation ability that centers around the expression of ALP.

2.3.3. Chronic dexamethasone exposure promotes the *in vitro* proliferation of MSCs in a concentration-dependent manner

I next analyzed how different concentrations of glucocorticoids (1 nM, 10 nM, or 100 nM dexamethasone) affect AT-MSCs differentiation. In all dosage conditions, AT-MSCs showed fibroblastic morphology and no morphological change was

observed between glucocorticoid-treated and untreated AT-MSCs (Fig. 5A). However, contrary to adipose-derived rat stromal cells reported previously (Sanderson, Sadie-Van Gijsen, Hough, & Ferris, 2015), dexamethasone promoted AT-MSCs proliferative activity in a concentration-dependent manner (Doubling time: no Dex, 50.4 ± 7.17 h; 1 nM, 35.7 ± 5.37 h; 10 nM, 28.2 ± 4.76 h, and 100 nM, 29.1 ± 7.14 h) (Fig. 5B, C). In addition, there was no difference in the MSC-like immune phenotype (in all conditions, AT-MSCs were positive for CD13, CD73, CD90, CD105, CD166, HLA-ABC, and negative for CD14, CD31, CD34, CD45, and HLA-DR) (Fig. 5D). Thus, dexamethasone-treatment affected only proliferative capacity but not the immune phenotype of AT-MSCs.

2.3.4. Chronic dexamethasone treatment impairs the *in vitro* osteogenic differentiation ability of MSCs

I next analyzed how glucocorticoids influence AT-MSCs differentiation ability towards osteogenic, adipogenic and chondrogenic lineages. Significant reduction of osteogenic differentiation ability was observed in dexamethasone-treated nAT-MSCs compared with untreated nAT-MSCs in a concentration-dependent manner (Day14: 1 nM, 0.82-fold; 10 nM, 0.67-fold; 100 nM, 0.3-fold, Day21: 1 nM, 0.92-fold, 10 nM, 0.70-fold; 100 nM, 0.44-fold vs No Dex)(Fig. 6A, B), whereas slight reduction of adipogenic and chondrogenic differentiation ability was observed in dexamethasone-treated nAT-MSCs (Fig. 6 C-F).

To clarify how the osteogenic differentiation mechanism was suppressed by the treatment of dexamethasone in nAT-MSCs, osteogenic-related genes were analyzed 7 and 14 days post-differentiation. As shown in Fig. 6G, alkaline phosphatase (ALP) gene expression was decreased concomitant to concentration increases of dexamethasone. In addition, expression of Runx2 and Osteocalcin were also downregulated in the presence of dexamethasone. I next examined the enzymatic activity of ALP by alkaline phosphatase staining and found that 100 nM dexamethasone-treated nAT-MSCs showed impaired ALP activity at 14 days post-differentiation (Fig. 6H). In addition, BMP-2, which promotes bone regeneration, was also downregulated in a concentration-dependent manner to increases of dexamethasone (Fig. 6I).

Taken together, these data indicated that continuous dexamethasone treatment of nAT-MSCs *in vitro* impaired their osteogenic differentiation ability, consistent with the impaired expression of ALP and other bone regeneration-related genes.

2.3.5. Alkaline phosphatase is downregulated through impairment of wnt/β-catenin signaling via high levels of Dkk-1

Previous studies have demonstrated that ALP plays a central role in calcification of the extracellular matrix (Hessle et al., 2002). The wnt/β-catenin signal pathway is known as a regulator of ALP expression (Rawadi, Vayssière, Dunn,

Baron, & Roman-Roman, 2003). Activation of the wnt/β-catenin signal pathway causes an accumulation of β-catenin that acts as a transcriptional coactivator of transcription factors that belong to the TCF/LEF family (Clevers, 2006). Therefore, I hypothesized that lower activation of wnt/β-catenin signaling might cause the impairment of β-catenin accumulation and lower ALP expression. To test this hypothesis, I examined the protein expression of β-catenin and found that β-catenin was downregulated in sAT-MSCs compared with nAT-MSCs (Fig. 7A).

Dickkopf1 (Dkk-1) is known as a wnt signal antagonist and the expression of Dkk-1 is upregulated by glucocorticoid treatment through a glucocorticoid-responsive element (GRE) located in the promoter region of Dkk-1 in osteoblasts (Etheridge, Spencer, Heath, & Genever, 2004; Ohnaka et al., 2004). In this study, I found that sAT-MSCs showed a higher expression of Dkk-1 protein compared to nAT-MSCs (Fig. 7B). I next examined whether Dkk-1 plays a central role in impairing osteogenic differentiation potential *in vitro* using shRNA of Dkk-1 in sAT-MSCs. Dkk-1 shRNA (shDkk-1)-transfected sAT-MSCs showed a significant reduction in Dkk-1 mRNA expression during osteogenic differentiation (Day 0: 0.059 ± 0.013-fold; Day 7: 0.15 ± 0.053-fold, Day 14: 0.16 ± 0.070-fold vs mock, Fig. 7C), whereas the expression of β-catenin was upregulated by Dkk-1 knockdown on day 14 (2.4 ± 0.67-fold vs mock) (Fig. 7D). During osteogenesis, shDkk-1-transfected sAT-MSCs showed recovered ALP gene expression and enzymatic activity (Fig. 7E, F). In addition, it should be

noted that osteogenic ability was also rescued by Dkk-1 knockdown in sAT-MSCs (Fig. 7F, G). On the other hand, the other osteogenic markers including Runx2, Osteocalcin, and Osteopontin, and BMP-2 were not changed by Dkk-1 knockdown (Fig. 7H, I).

Next, I examined whether dexamethasone-treated nAT-MSCs could have their osteogenic ability rescued by modulating wnt/β-catenin signaling. Interestingly, I found that dexamethasone treatment resulted in both in downregulation of β-catenin and upregulation of Dkk-1 expression (Fig. 8A, B). Subsequently, I examined whether an inhibitor of Dkk-1, way262611, could rescue the impaired osteogenesis. I found the administration of way262611 (0.4 μg/ml) promoted the suppression of osteogenic differentiation (Fig. 8C). Previous studies have reported that a wnt/β-catenin signal suppresses osteogenesis in MSCs, whereas the differentiation of osteoblasts is promoted through wnt/β-catenin signaling (de Boer et al., 2004; Gaur et al., 2005). Therefore, the Dkk-1 inhibitor, way262611, might affect cell fate when the osteogenic linage has already committed to osteoblast. To test this hypothesis, I next examined whether the osteogenesis in dexamethasone-treated nAT-MSCs is rescued by adding way262611 at day 7 of osteogenic differentiation, after the expression of Dkk-1 would be already upregulated (Fig. 8B). Of note, the elevation of β-catenin protein expression was confirmed on day 14 in the presence of way262611 (Fig. 8D). I also examined ALP activity and osteogenic differentiation ability and found that both ALP activity and osteogenesis in

dexamethasone-treated MSCs were recovered on day 21 in the presence of way262611 at the level of the control (Fig. 8E, F). By contrast, other osteogenic differentiation markers and BMP-2 were not changed in the presence of way262611 consistent with the result in shDkk-1-transfected sAT-MSCs (Fig. 8G, H)

Collectively, these data demonstrate that high expression of Dkk-1 in sAT-MSCs downregulates wnt/β-catenin signaling, resulting in the impairment of osteogenic ability. In addition, these inhibitory effects can be reversed with a Dkk-1 inhibitor after the MSCs commit to the osteoblast lineage.

2.3.6. Lowered bone regeneration capacity of sAT-MSCs was reversed by shDkk1

The impaired expression of osteogenesis-related and bone regenerative factors in sAT-MSCs suggested that sAT-MSCs might have less bone regenerative capacity than nAT-MSCs, possibly because of the overexpression of Dkk-1. I, therefore, examined the bone regenerative capacity of nAT-MSCs, sAT-MSCs, nAT-MSCs transfected with mock, sAT-MSCs transfected with mock and sAT-MSCs transfected with shDkk-1, using the critical-sized calvarial defect mouse model (Cowan et al., 2004). As previously reported, nAT-MSCs, and mock-transfected nAT-MSCs could facilitate bone formation whereas sAT-MSCs showed impaired bone regenerative capacity (Ko et al., 2016; Xie et al., 2016). In contrast, shDkk-1-transfected sAT-MSCs showed significant increases in

bone regenerative capacity compared with the sAT-MSCs transfected with mock (Fig. 9A, B). Similarly, H & E staining of injured skulls showed that nAT-MSCs, mock-transfected nAT-MSCs and shDkk-1-transfected sAT-MSCs enhanced new bone formation which could not be observed in mock sAT-MSCs (Fig. 9C). To prove the presence of transplanted AT-MSCs in the repaired bone regions, I performed immunohistological analyses using anti-human osteopontin (hOPN) antibody. Intriguingly, I found there were hOPN-positive cells in the repaired bone regions with nAT-MSCs, mock-transfected nAT-MSCs or shDkk-1-transfected sAT-MSCs. In contrast, no positive cells were observed in sAT-MSCs or mock-transfected sAT-MSCs at the transplanted regions (Fig. 9D).

Thus, these data strongly indicate that continuous glucocorticoid therapy impaired the osteogenic and bone regenerative capacity of AT-MSCs because of upregulation of Dkk-1 expression.

I next investigated whether plasma Dkk-1 may reflect steroid-induced ONFH progression. ELISA analysis clearly showed increased level of Dkk-1 in steroid-induced ONFH patient plasma compared with non-steroid-treated ONFH patients (non-steroidal: 955.8±328.6, steroidal: 1375.8±397.4, 1.44-fold, Fig. 10). Thus, the present data shown in this thesis indicates that plasma Dkk-1 levels may likely predict side effects in steroid-induced ONFH patients. However, more precise analysis is required to clarify the mechanism how Dkk-1 affects the overall condition of steroid-induced ONFH patients.

2.4. Discussion

In this study, I demonstrated that BM-MSCs from steroid-induced ONFH patients showed less self-renewal and proliferative ability compared with those of traumatic ONFH patients. Chronic glucocorticoid treatment impaired the osteogenic and bone regenerative capacity of AT-MSCs because of highly upregulation of Dkk-1 expression, which antagonizes wnt/β-catenin signalling. The reduced expression of ALP was also observed in sAT-MSCs, possibly because of the impaired expression of β-catenin. Consistent with these findings, higher expression of Dkk-1 was measured in the plasma from steroid-induced ONFH patients versus traumatic ONFH patients (Fig, 11).

ONFH is characterized by bone tissue ischemia which leads to death of osteocytes (Jones & Hungerford, 2004; Urbaniak et al., 1995). Approximately 51% patients with ONFH have received glucocorticoid therapy and long term or pulsed glucocorticoid treatments for severe respiratory syndrome, rheumatoid diseases, and organ transplantation increase the risk of ONFH (Fukushima et al., 2010). Autologous BM transplantation has been reported as a novel approach to treat ONFH (Yoshioka et al., 2011). In this therapy, transplanted whole BM-derived cells, including MSCs, promote bone regeneration and this therapeutic outcome is thought to be correlated with the number of transplanted MSCs (Gangji, De Maertelaer, & Hauzeur, 2011; Philippe Hernigou & Beaujean, 2002; Sen et al., 2012). In this study, I demonstrated that the number and

proliferative ability of BM-MSCs from steroid-induced ONFH patients was impaired compared with traumatic ONFH patients and cultured BM-MSCs displayed unstable growth as previously reported (Houdek et al., 2016; Wang et al., 2008). Thus, autologous cell therapy using BM-MSCs from steroid-induced ONFH patients may not achieve critical cell thresholds due to their impaired proliferative activity.

As an alternative cell source, AT-MSCs are attractive because of their abundance, proliferative activity, and lower invasiveness compared with BM-MSCs. As shown in Fig. 1, BM-MSCs-derived from ONFH patients have less proliferative activity, suggesting that cell therapy using AT-MSCs would be appropriate for steroid-induced ONFH patients. Consistent with these results, previous reports showed that AT-MSCs-derived from ONFH patients have higher proliferative and osteogenic potential compared with BM-MSCs (Wyles et al., 2015). Therefore, AT-MSCs are a more robust source for cell therapy rather than BM-MSCs. However, no study has performed the comparative analysis of AT-MSCs derived from both traumatic and steroid-induced ONFH patients. Intriguingly, sAT-MSCs showed the same proliferative ability as nAT-MSCs (Fig. 2B, C). On the other hand, nAT-MSCs treated continuously by dexamethasone (mimicking the microenvironment of AT-MSCs in steroid-induced ONFH patients) showed a concentration-dependent proliferative ability (Fig. 5B, C), indicating that glucocorticoid treatment does not affect AT-MSCs proliferative ability. In addition, sAT-MSCs did not show any significant difference in

adipogenesis compared with nAT-MSCs (Fig. 3C, D) although previous studies demonstrated that glucocorticoid treatment upregulated the expression of adipogenic genes including PPARγ and lipoprotein lipase (LPL) and facilitated adipogenesis *in vitro* (Cooper & Hardy, 2011). However, other previous study showed steroid-induced ONFH patient-derived BM-MSCs did not show significant change in adipogenesis compared with osteoarthritis patient-derived BM-MSCs that was consistent with present results shown in this thesis (Fig. 3C, D) (Lee et al., 2006). Therefore, chronic glucocorticoid treatment to patients might not affect the adipogenic differentiation ability of MSCs.

It has been reported that several signaling pathways, such as p38/MAPK signaling and wnt/β-catenin signaling, are involved in chondrogenesis, osteogenesis, and regulation of ALP expression (Marie, 2008; Rawadi et al., 2003; X. Shao et al., 2017; X. R. Shao et al., 2017; Suzuki, Palmer, Bonjour, & Caverzasio, 1999). In particular, the wnt/β-catenin signaling pathway is associated with osteogenesis and ALP expression independent of Runx2 and Osteocalcin expression (Rawadi et al., 2003). Moreover, several studies have reported that wnt antagonists including WIF-1, SOST, and Dkk-1 were upregulated by glucocorticoids (Hayashi et al., 2009; Yao, Cheng, Pham, et al., 2008). Based on these findings, I found that wnt/β-catenin signaling was suppressed by highly expressed Dkk-1 during osteogenesis (Fig. 7, 8). In addition, the expression of bone regenerative cytokines, such as BMP-2, was reduced compared with the control, and the expression of BMP-2 was not

recovered even the expression of Dkk-1 was diminished (Fig. 4E, 6I, 7I, 8H), clearly indicating that BMP-2 expression was not related with Dkk-1 expression.

ALP is also known to play a central role in mineralization of the extracellular matrix (Orimo, 2010). ALP knockout mice display skeletal defects of infantile hypophosphatasia and osteoblasts derived from ALP knockout mice showed no calcification ability (Fedde et al., 1999; Wennberg et al., 2000). In addition, previous studies have reported that ALP activity in serum was correlated with bone healing processes (Cox, Einhorn, Tzioupis, & Giannoudis, 2010; Mukhopadhyay et al., 2011; Muljacic et al., 2013; Stucki, Schmid, Hammerle, & Lang, 2001). In this study, I demonstrated that the downregulation of ALP in sAT-MSCs caused reduced osteogenic differentiation ability and sAT-MSCs transfected with Dkk-1 shRNA showed ALP upregulation and restored osteogenic differentiation (Fig. 4D, 7E-G). Thus, the expression of ALP may be critical for not only osteogenesis *in vitro* but also bone healing *in vivo*. Further analysis is therefore required to understand the precise physiological mechanisms of ALP during bone regeneration.

In addition to ALP, BMP-2 is also known as an important factor for osteogenesis and bone repair (Salazar, Gamer, & Rosen, 2016). During osteogenic differentiation, BMP-2 regulates key transcription factors, such as Runx2 and Osterix, that induce downstream gene expression of Osteocalcin and type 1 collagen (Matsubara et al., 2008). In sAT-MSCs, the expression level of BMP-2 was decreased and knockdown of Dkk-1 expression did not affect BMP-2

expression even if osteogenic ability was restored (Fig.7I), suggesting that in osteogenic differentiation medium, dexamethasone, β-glycerophosphate, and ascorbic acid induce the expression of Runx2 and type 1 collagen in the absence of BMP-2 (Langenbach & Handschel, 2013). In fact, osteoblasts derived from BMP-2 knockout mice showed less osteogenic ability but still they possess osteogenic potential (Wu et al., 2016). In sAT-MSCs, reduced BMP-2 expression showed impaired osteogenic ability, however, the expression level of Runx2 and Osteocalcin was not significantly changed compared with nAT-MSCs (Fig. 4A). These results suggest that the major reason for reduced osteogenic differentiation ability in sAT-MSCs is reduced ALP expression, resulting in calcification inhibition. On the other hand, previous studies demonstrated that secretion of BMP-2 by AT-MSCs promotes bone repair by stimulating endogenous osteoblasts and MSC differentiation (H. Li et al., 2007; Tsuji et al., 2006). As shown in Fig. 9D, transplanted AT-MSCs differentiated into mature osteoblasts *in vivo,* however, human osteopontin-positive osteoblasts were not abundant in the bone defect region. These results suggest that both beneficial effects, such as differentiation into osteoblasts and cytokine secretion (including BMP-2) would be required for effective bone repair. Thus, supplementation of BMP-2 in addition to the diminished expression of Dkk-1 in sAT-MSCs may result in more effective bone repair.

Dkk-1 is a wnt signaling antagonist often associated with bone physiology and Dkk-1 overexpressing mice are reported to show severe

osteopenia (J. Li et al., 2006). In addition, several studies have clearly showed high levels of Dkk-1 in plasma are associated with rheumatoid arthritis, osteoarthritis, bone mineral density, and osteolytic lesions in multiple myeloma (Butler et al., 2011; Diarra et al., 2007; Honsawek et al., 2010; Tian et al., 2003). In this study, it was noted that the upregulation of Dkk-1 was observed in plasma derived from steroid-induced ONFH patients versus non-steroid-treated patients (Fig. 10). Excess glucocorticoid treatment also caused increased expression of Dkk-1 in murine BM cells and osteoblasts (Ohnaka et al., 2004; Yao, Cheng, Busse, et al., 2008), suggesting that highly expressed Dkk-1 would be involved in the pathogenesis of steroid-induced ONFH.

In conclusion, I demonstrated that glucocorticoid treatment impairs the proliferative potential of BM-MSCs whereas proliferation in AT-MSCs derived from steroid-induced ONFH patients were not affected. On the other hand, the osteogenic ability of sAT-MSCs was affected through the downregulation of wnt/β-catenin signaling because of highly expressed Dkk-1. Long-term treatment with glucocorticoids may therefore reduce the therapeutic function of AT-MSCs. In addition, it was noted that higher levels of Dkk-1 were also observed in the plasma from steroid-induced ONFH patients, suggesting Dkk-1 expression would be key promoter of AT-MSCs as a useful therapy source instead of BM-MSCs. Taken together, in the treatment of steroid-induced ONFH, transplantation of BM-MSCs is not effective due to lower cell numbers with lower proliferative activity whereas AT-MSCs would be more useful if combined with

downregulation of Dkk-1 expression.

2.5. Tables and Figures

Table 1. The primer sets for polymerase chain reactions used in chapter 2

		Sequence
β-actin	Forword	GTGCGTGACATTAAGGAGAAGCTGTGC
	Reverse	GTACTTGCGCTCAGGAGGAGCAATGAT
Runx2	Forword	CATCCCAGTATGAGAGTAGGTG
	Reverse	GGGTCTGTAATCTGACTCTGTC
ALP	Forword	TCAAACCGAGACACAAGCAC
	Reverse	TCACGTTGTTCCTGTTCAGC
Osteocalcin	Forword	AATCCGGACTGTGACGAGTT
	Reverse	CAAGGGGAAGAGGAAAGAAG
Osteopontin	Forword	ACTCGAACGACTCTGATGATGT
	Reverse	GTCAGGTCTGCGAAACTTCTTA
Dkk-1	Forword	TGTTTGTCTCCGGTCATCAG
	Reverse	TCCATGAGAGCCTTTTCTCC

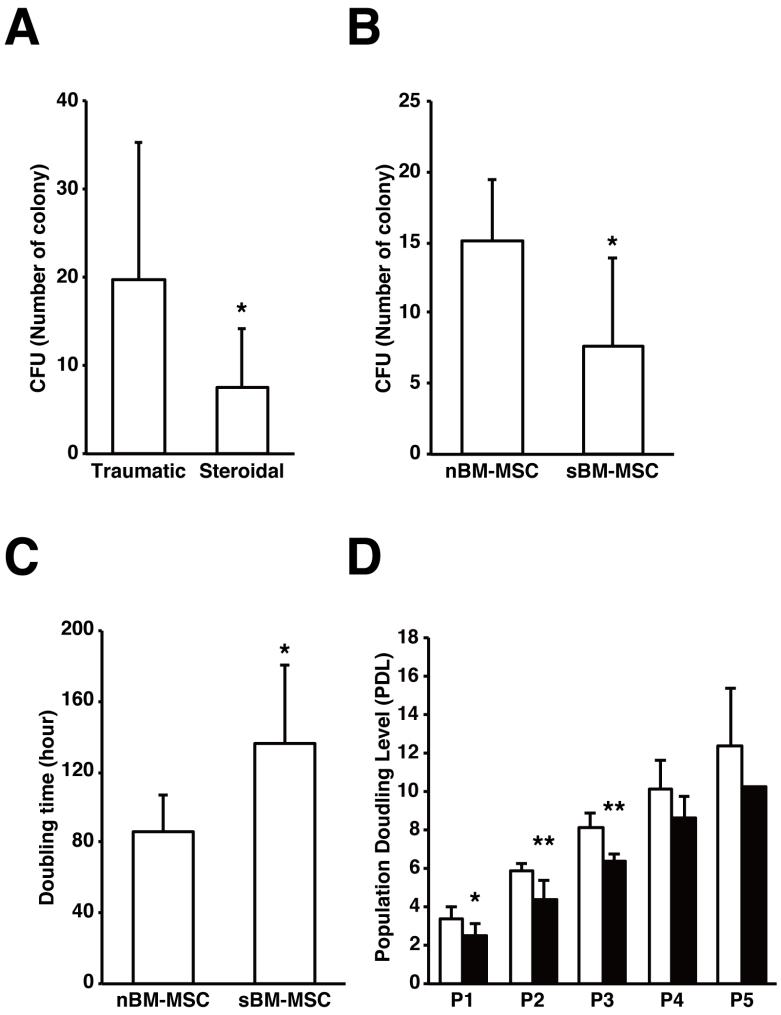

Figure 1. Chronic glucocorticoid treatment impaired mesenchymal stem cell pool in bone marrow and their proliferation potential *in vitro*.

(A): Fibroblast Colony Forming Unit (CFU-F) was evaluated using primary bone marrow aspirate (p0). The bone marrow from steroid-induced ONFH patients showed significant lower number of colony than traumatic ONFH patients. Steroid: N=36, Traumatic: N=12, *P < 0.05. (B): CFU-F of bone marrow derived mesenchymal stem cells from steroid-induced (sBM-MSC) or traumatic (nBM-MSC) ONFH patients was analyzed at P1 *in vitro*. nBM-MSC showed significant higher number colony than sBM-MSC. nBM-MSC; N=5, sBM-MSC; N=5, *P < 0.05. (C): Doubling time of each nBM-MSC and sBM-MSC. sBM-MSC

showed less doubling time than nBM-MSC. nBM-MSC; N=5, sBM-MSC; N=5, *P < 0.05. (D): Population doubling level (PDL) was evaluated in nBM-MSC and sBM-MSC until passage 5. nBM-MSC: P1, N=5; P2, N=5; P3, N=5; P4, N=5; P5, N=3. sBM-MSC; P1, N=13, P2; N=9, P3; N=4, P4; N=2, P5; N=1. *P < 0.05, **P < 0.01.

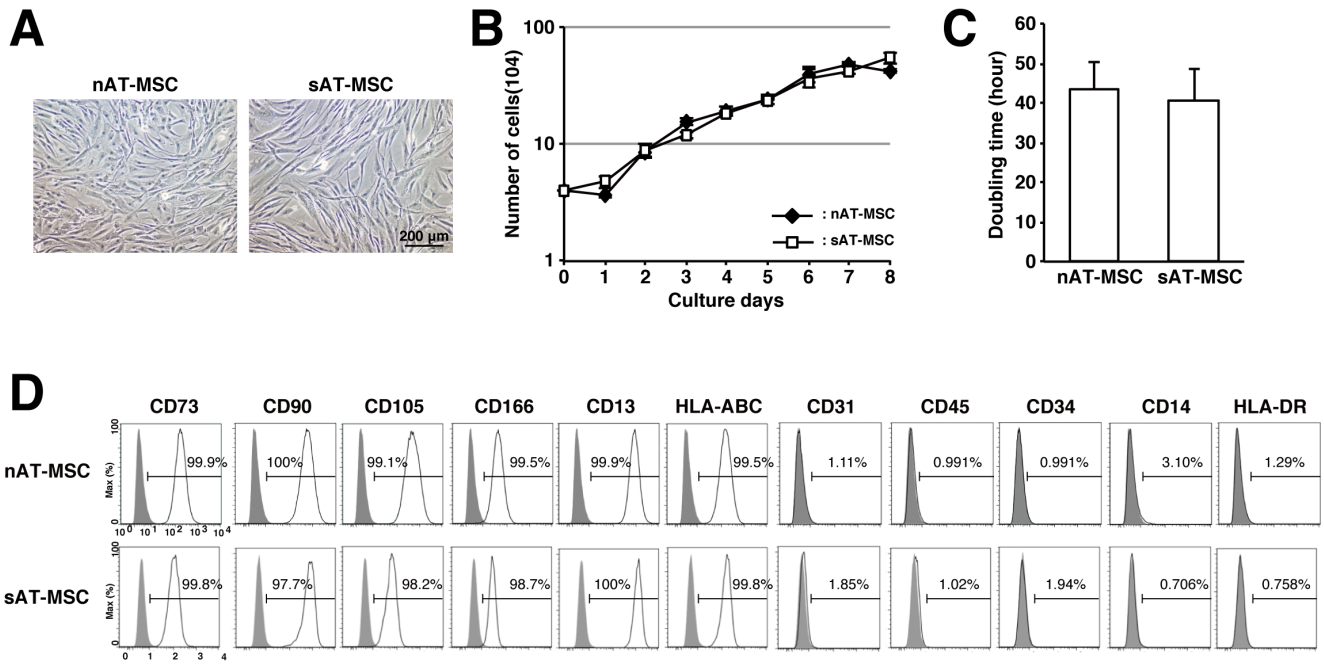

Figure 2. Isolation of Mesenchymal stem cells from traumatic and steroid-induced ONFH patients

(A): The morphology of nAT-MSCs and sAT-MSCs cultured in maintenance medium. Scale bar indicates 200 μm. (B, C): nAT-MSCs and sAT-MSCs were incubated and harvested every 24 hours until the cultures reached confluence. Doubling time is calculated from day 2 to 5 and the mean ± SD was obtained from triplicate wells. N=3. (D): Expression analysis of cell surface antigens. FACS analysis of cell surface markers on nAT-MSCs or sAT-MSCs was analyzed for the expression of cell surface markers (CD13, CD14, CD31, CD34, CD45, CD73, CD90, CD105, CD166, HLA-DR, and HLA-ABC).

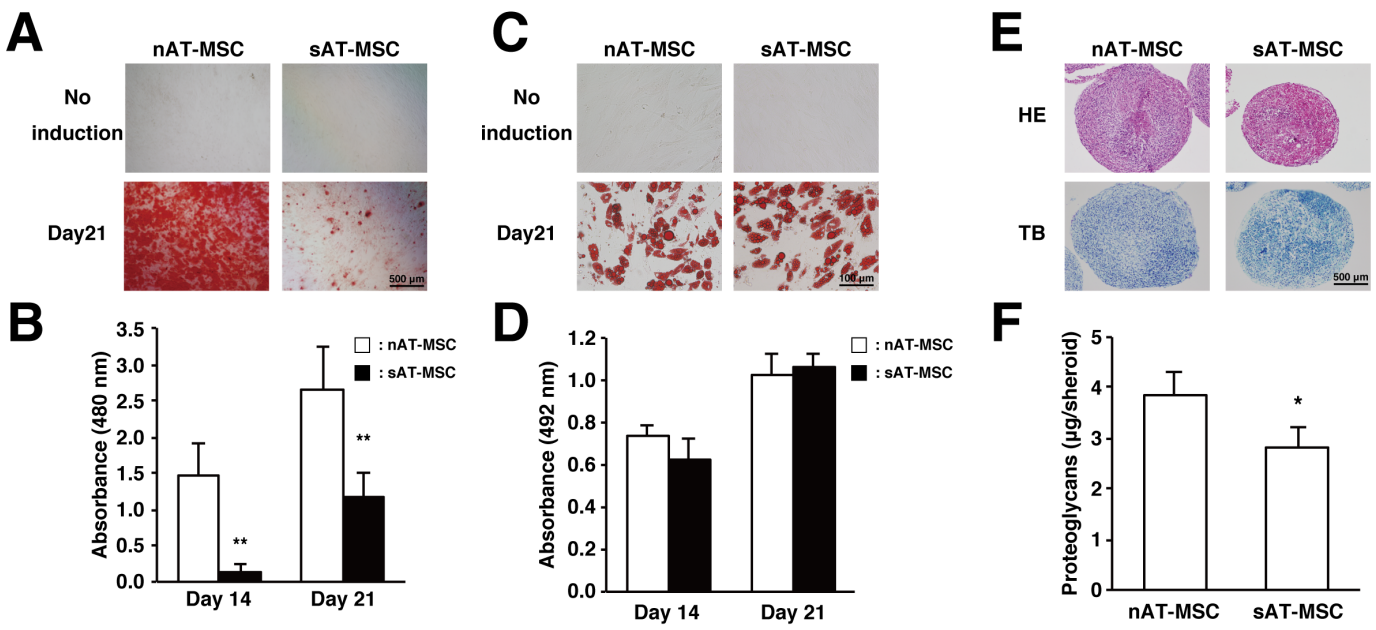

Figure 3. Analysis of the differentiation potential of nAT-MSC and sAT-MSC *in vitro*

(A, B): The osteogenic differentiation of nAT-MSCs and sAT-MSCs were determined by Alizarin Red S staining in controls or at day 21 post-induction. After staining, the absorbances of each AT-MSCs were measured at day 14 and 21. Scale bar indicates 500 μm. White column, nAT-MSCs; Black column, sAT-MSCs. N=6, **P<0.01, ANOVA with Tukey-Kramer multiple comparison test. (C, D): The adipogenic differentiation of nAT-MSCs and sAT-MSCs were analyzed by Oil Red O staining of lipid vacuoles. Absorbances were recorded and data were presented as described in (F). Scale bar indicates 100 μm, N=6, ANOVA with Tukey-Kramer multiple comparison test. (E, F):Chondrogenic differentiation was examined by toluidine blue staining. Scale bar indicates 500

μm. Proteoglycan levels of spheroids were examined by use of a mucopolysaccharide assay kit. N=6, *P<0.05, Student's *t*-test.

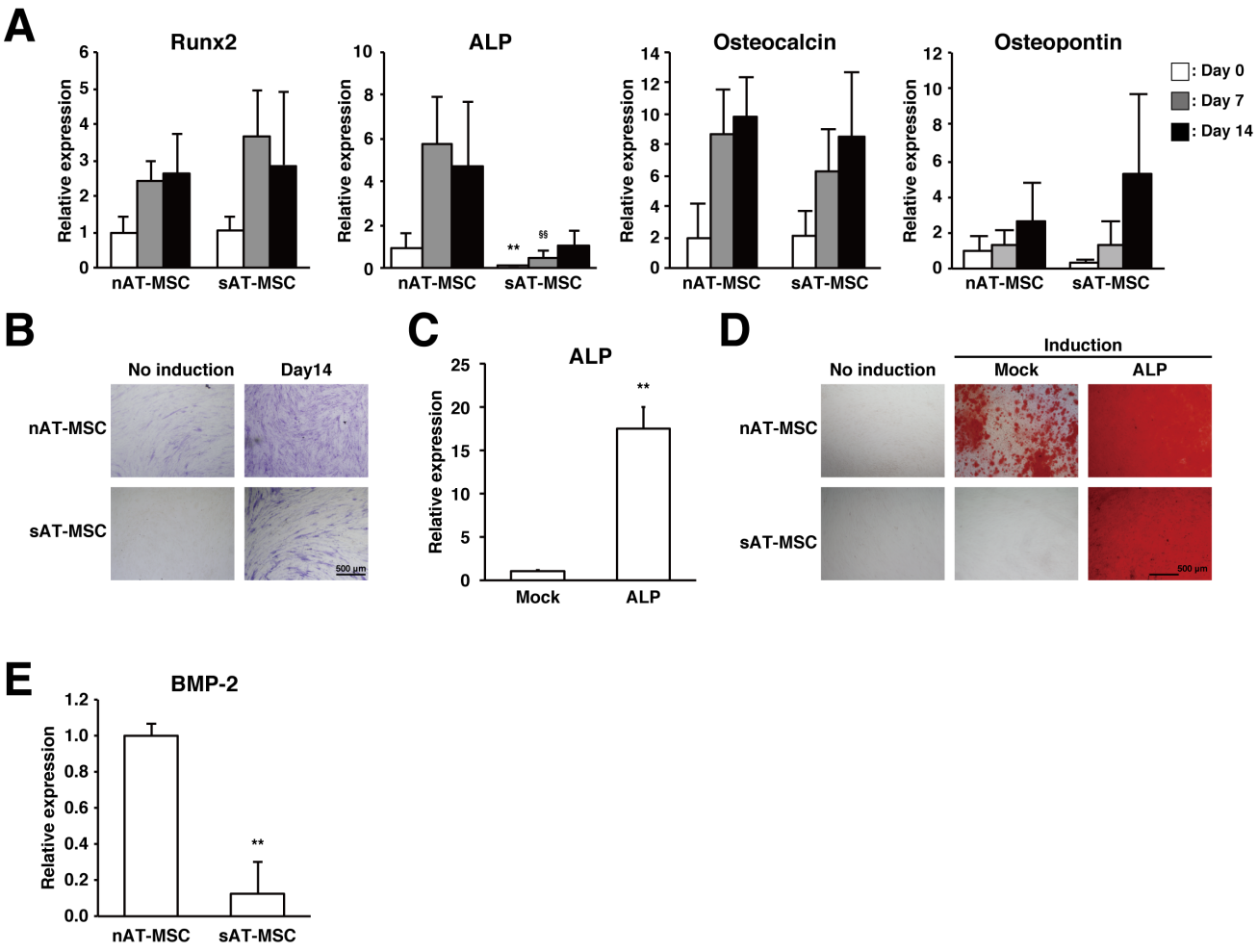

Figure 4. Figure 4. Analysis of osteogenic markers in nAT-MSC and sAT-MSC

(A): The expression of genes related to osteogenic differentiation was measured by qPCR in controls versus day 7 and 14 post-differentiation. The relative units of expression in each culture condition are shown and the data obtained from nAT-MSCs at day 0 were normalized to a value of 1 as the standard. White column, day 0; gray column, day 7; black, day 14. N=6, **P<0.01 (nAT-MSC vs sAT-MSC on day 0); §§P<0.01 (nAT-MSC vs sAT-MSC on day 7), ANOVA with Tukey-Kramer multiple comparison test. (B): The enzymatic activity of alkaline

phosphatase was analyzed by alkaline phosphatase staining at day 14. Scale bar indicates 500 μm. (C): The gene expression of alkaline phosphatase was measured by qPCR in mock-transfected sAT-MSC and ALP overexpressed sAT-MSC at day 0. The relative units of expression were shown and the data obtained from mock-transfected sAT-MSCs at day 0 were normalized to a value of 1 as the standard. N=3, **P<0.01, Student's *t*-test. (D): The osteogenic differentiation of sAT-MSCs overexpressing alkaline phosphatase versus mock was determined by Alizarin Red S staining or alkaline phosphatase staining in controls and at day 14 post-induction. Scale bar indicates 500 μm. (E): The gene expression of BMP-2 was measured by qPCR. The relative units of expression were shown and the data obtained from nAT-MSC was normalized to a value of 1 as the standard. N=3, **P<0.01, Student's *t*-test.

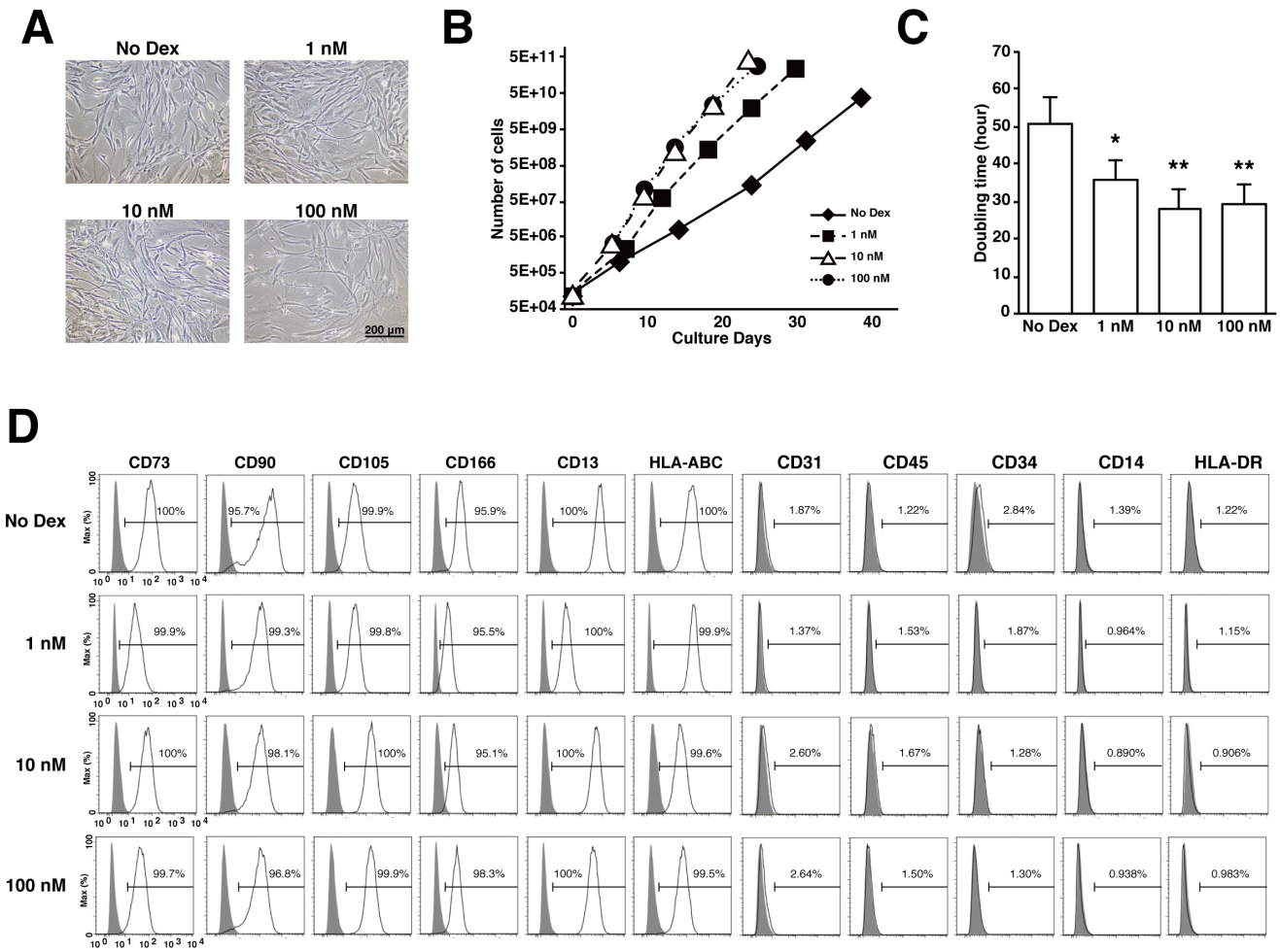

Figure 5. Characterization of nAT-MSC exposed to chronic dexamethasone *in vitro*

(A): AT-MSCs morphology cultured in each dexamethasone concentration after five passages. Scale bar indicates 200 μm. (B, C): Cell proliferative activity during dexamethasone exposure from P0 to P5. N=3, *P < 0.05, **P < 0.01, ANOVA with Tukey-Kramer multiple comparison test. (D): Expression analysis of cell surface antigens. FACS analysis of cell surface markers on AT-MSCs cultured in each dexamethasone concentration was analyzed for the expression

of cell surface markers (CD13, CD14, CD31, CD34, CD45, CD73, CD90, CD105 CD166, HLA-DR, and HLA-ABC). These MSC expressed characteristic MSC markers (including CD73, CD90, and CD105) but lacked expression of hematopoietic linage and endothelial makers.

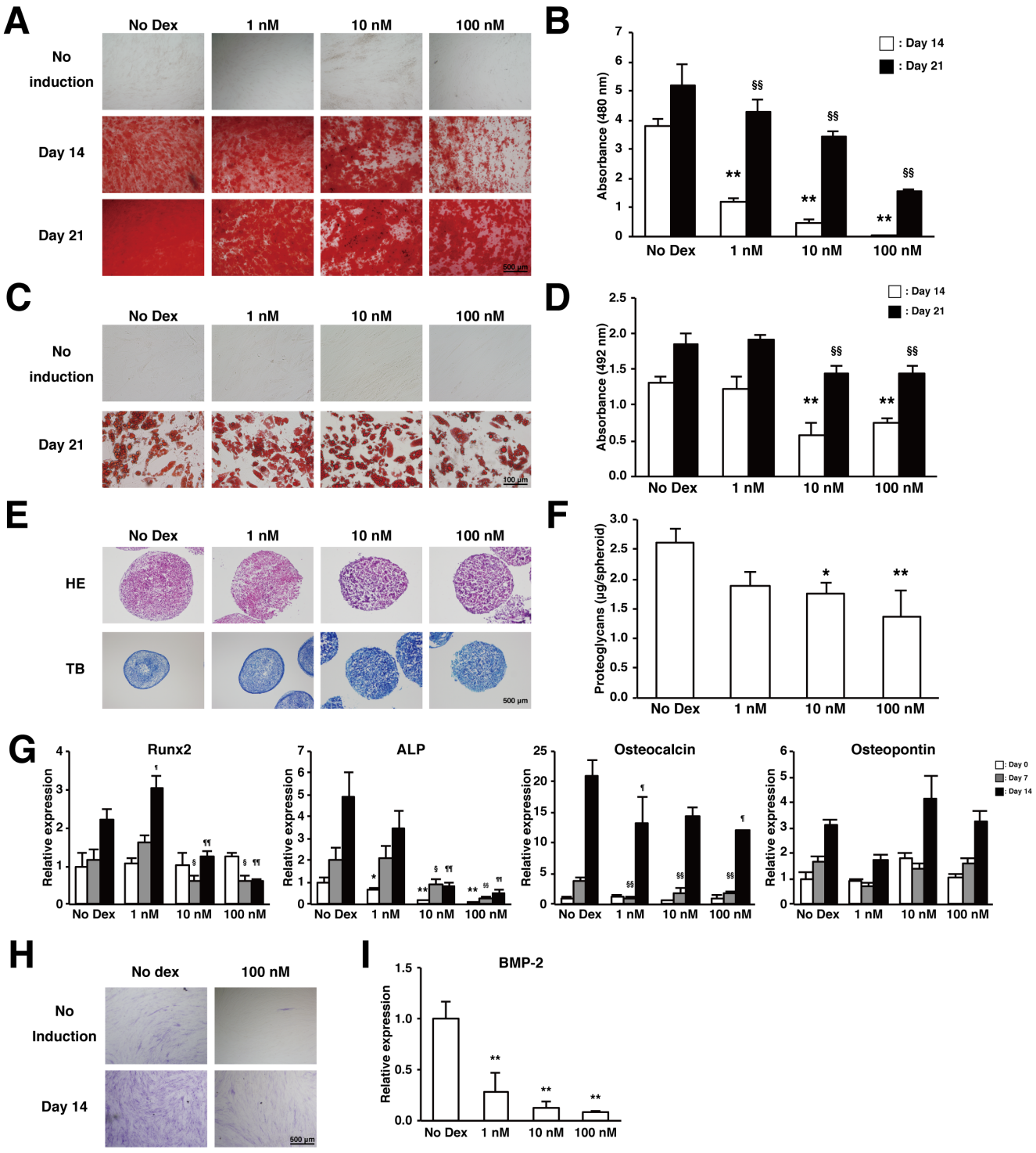

Figure 6. Characterization of AT-MSCs exposed to dexamethasone

(A, B): The osteogenic differentiation of AT-MSCs cultured in differing dexamethasone concentrations was determined by Alizarin Red S staining in controls and day 14 and 21 post-induction. Scale bar indicates 500 μm. After

staining, absorbances were measured at each time point. White column, day 14; black, day 21, N=3, **P<0.01 (No dex vs the others on day 14); §§P<0.01 (No Dex vs the others on day 21), ANOVA with Tukey-Kramer multiple comparison test. (C, D): The adipogenic differentiation of AT-MSCs cultured in differing dexamethasone concentrations was analyzed by Oil Red O staining of lipid vacuoles. Scale bar indicates 100 μm. Absorbances were measured and data were presented as described in (A). N=3, **P<0.01 (No dex vs the others on day 7); §§P<0.01 (No Dex vs the others on day 7), ANOVA with Tukey-Kramer multiple comparison test. (E, F): Chondrogenic differentiation was examined by toluidine blue staining. Scale bar indicates 500 μm. Proteoglycan level of spheroids were examined by use of a mucopolysaccharide assay kit. N=3, *P<0.05, **P<0.01, ANOVA with Tukey-Kramer multiple comparison test. (G): The expression of genes related to osteogenic differentiation was measured by qPCR in controls versus day 7 and 14 post-differentiation. The relative units of expression in each culture condition are shown and the data obtained from AT-MSCs cultured under no dexamethasone conditions were normalized to a value of 1 as the standard. White column, day 0; gray column, day 7; black, day 14. N=3, *P<0.05, **P<0.01 (No dex vs the others on day 0); §P<0.05, §§P<0.01 (No Dex vs the others on day 7); ¶P<0.05, ¶¶P<0.01 (No Dex vs the others on day 14), ANOVA with Tukey-Kramer multiple comparison test. (H): The enzymatic activity of alkaline phosphatase was analyzed by alkaline phosphatase staining at day 14. Scale bar indicates 500 μm. (I): The gene expression of BMP-2 was

measured by qPCR at day 0. The relative units of expression in each culture condition were shown and the data obtained from AT-MSCs cultured under no dexamethasone conditions were normalized to a value of 1 as the standard. N=3, *P<0.05, **P<0.01 (No dex vs the others), ANOVA with Tukey-Kramer multiple comparison test.

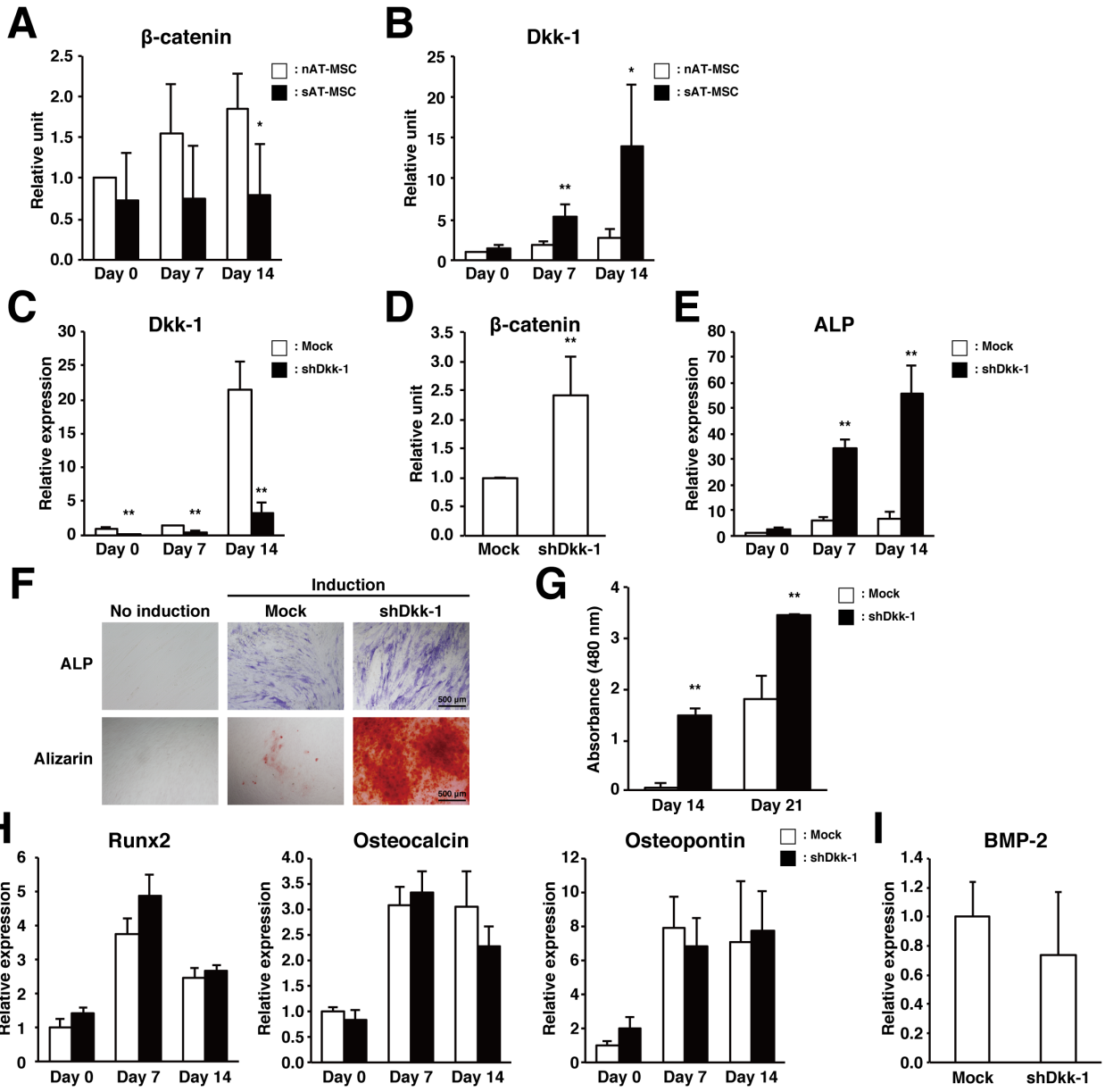

Figure 7. Wnt signaling was suppressed in sAT-MSCs via high levels of Dkk-1

(A, B): The protein expression levels of β-catenin and Dkk-1 were analyzed by western blot in nAT-MSCs or sAT-MSCs and the expression level in nAT-MSCs at day 0 was normalized to a value of 1. White column, nAT-MSC; black,

sAT-MSC, N=3, *p<0.05; **p<0.01, ANOVA with Tukey-Kramer multiple comparison test. (C): Dkk-1 gene expression levels were measured by qPCR in sAT-MSCs transfected with shDkk-1 or mock at day 0, 7, and 14. The relative units of expression are shown and the data obtained from sAT-MSCs transfected with mock plasmid at day 0 was normalized to a value of 1 as the standard. White column, sAT-MSC with mock; black, sAT-MSC with shDkk-1, N=3, *P<0.05, ANOVA with Tukey-Kramer multiple comparison test. (D): The protein expression level of β-catenin was analyzed by western blot in shDkk-1 sAT-MSCs or mock. The relative units of expression are shown and the data obtained from sAT-MSCs with vehicle at day 14 was normalized to a value of 1 as the standard. White column, mock; black, shDkk-1, N=3, *P<0.05, Student's *t*-test. (E): The expression of ALP was measured by qPCR in controls versus day 7 and 14 post-differentiation. The relative units of expression in each culture condition are shown and the data obtained from sAT-MSCs with mock at day 0 was normalized to a value of 1 as the standard. White column, mock; black, shDkk-1, N=3, **P<0.01, ANOVA with Tukey-Kramer multiple comparison test. (F, G): The osteogenic differentiation of shDkk-1 sAT-MSCs or mock was determined by Alizarin Res S staining or alkaline phosphatase staining in controls and at day 14 post-induction. Scale bar indicates 500 μm, N=3, **P<0.01, ANOVA with Tukey-Kramer multiple comparison test. (H): The expression of genes related osteogenesis were measured by qPCR. The relative units of expression were shown and the data obtained from sAT-MSCs

transfected with mock at day 0 was normalized to a value of 1 as the standard. N=3, ANOVA with Tukey-Kramer multiple comparison test. (I): The gene expression of BMP-2 was measured by qPCR. The relative units of expression were shown and the data obtained from sAT-MSCs transfected with mock was normalized to a value of 1 as the standard. N=3, **P<0.01, Student's t-test.

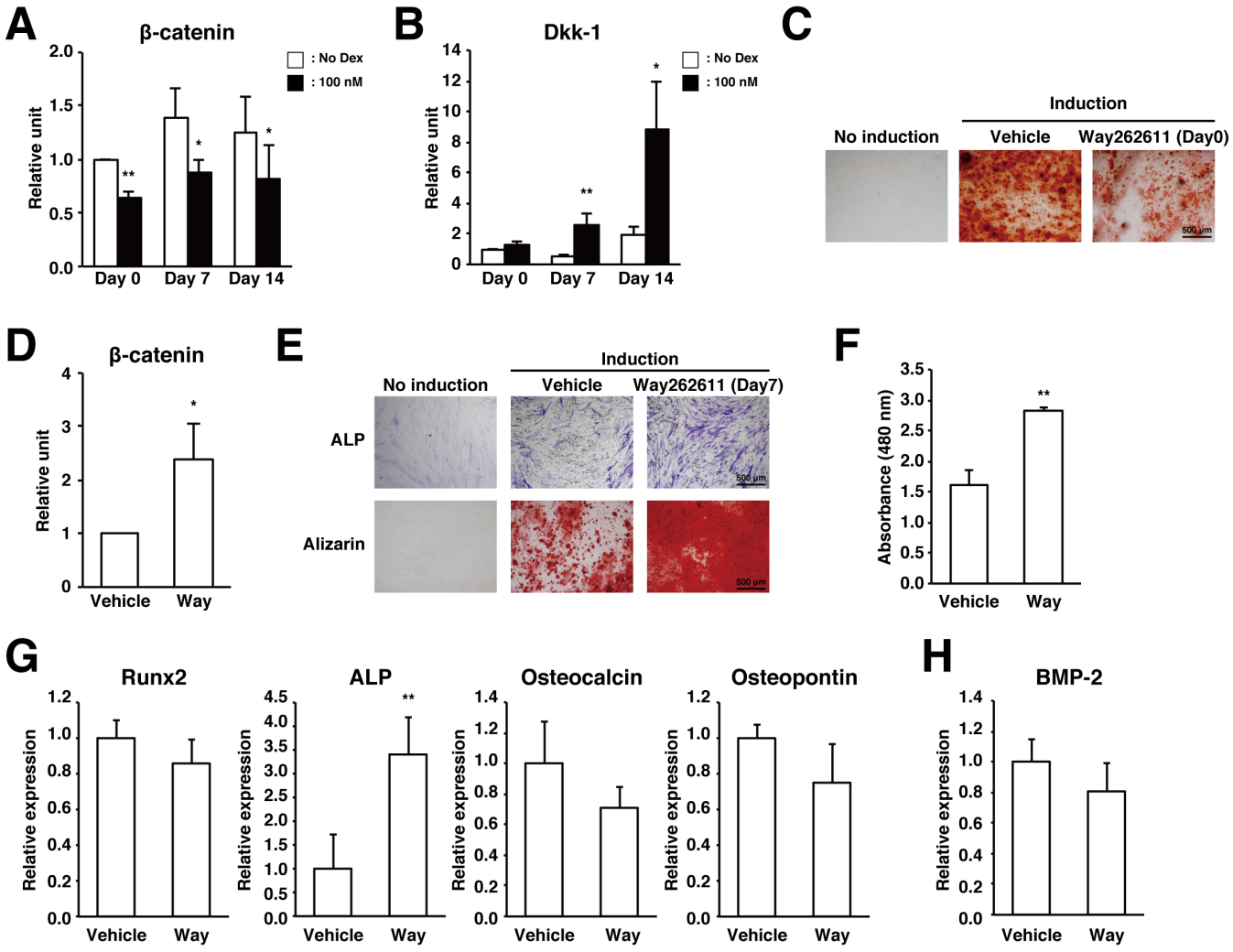

Figure 8. Inhibition of Dkk-1 improved impaired osteogenesis caused by dexamethasone treatment

(A, B): The protein expression levels of β-catenin and Dkk-1 were analyzed by western blot in AT-MSCs cultured without dexamethasone, or cultured with 100 nM dexamethasone. The expression level seen under the no dexamethasone condition at day 0 was normalized to a value of 1. White column, No Dex; black, 100 nM, *p<0.05; **p<0.01, ANOVA with Tukey-Kramer multiple comparison test.

(C): The osteogenic differentiation of AT-MSCs cultured with 100 nM dexamethasone and 0.4 μg/ml way262611 or vehicle (ethanol) administrated

from day 0 was determined by Alizarin Red S staining in controls or at day 14 post-induction. Scale bar indicates 500 μm. (D): The protein expression level of β-catenin was analyzed by western blot in 100 nM dexamethasone treated AT-MSCs with way262611 or vehicle. The relative units of expression are shown and the data obtained from 100 nM dexamethasone with vehicle at day 14 was normalized to a value of 1 as the standard. White column, vehicle; black, way262611, N=3, *P<0.05, Student's *t*-test. (E, F): The osteogenic differentiation of AT-MSCs cultured with 100 nM dexamethasone and 0.4 μg/ml way262611 or vehicle (ethanol) administrated from day 7 was determined by Alizarin Red S staining or alkaline phosphatase staining in controls or at day 14 post-induction. Scale bar indicates 500 μm. After staining, the absorbances of each AT-MSCs were measured. Left column, vehicle; right, 0.4 μg/ml way262611. N=3, **P<0.01, Student's *t*-test. (G): The expression of genes related osteogenesis were measured by qPCR. The relative units of expression are shown and the data obtained from nAT-MSCs cultured under the presence of 100 nM dexamethasone and vehicle (ethanol) was normalized to a value of 1 as the standard. N=3, **P < 0.01, Student's t-test. (H): The gene expression of BMP-2 was measured by qPCR. The relative units of expression were shown and the data obtained from nAT-MSCs cultured under the presence of 100 nM dexamethasone and vehicle was normalized to a value of 1 as the standard. N=3, Student's t-test.

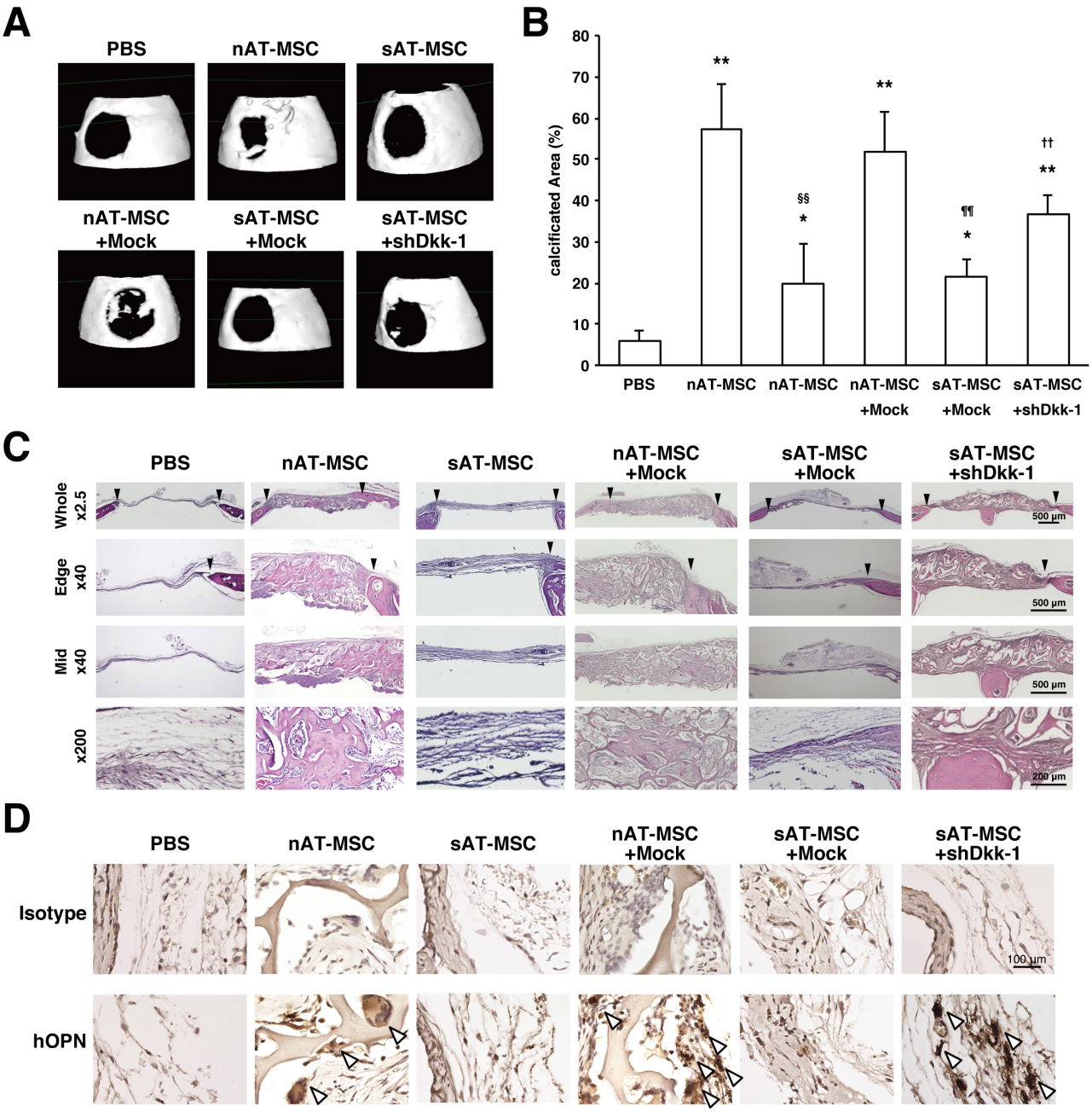

Figure 9. Lowered bone regeneration capacity of sAT-MSCs was reversed by shDkk1

(A): µCT analysis was performed at 3 month post transplantation of either nAT-MSC or sAT-MSC or nAT-MSC + Mock or sAT-MSC + Mock or sAT-MSC + shDkk-1 or PBS (scaffold without cells). (B): Graphic representation of the average bone volume within the defect for each group with standard deviations. N=5, *P < 0.05, **P < 0.01(PBS vs the others); §§P<0.01 (nAT-MSC vs

sAT-MSC); ¶¶P<0.01 (nAT-MSC+Mock vs sAT-MSC+Mock and sAT-MSC+shDkk-1); ††P<0.01 (sAT-MSC+Mock cs sAT-MSC+shDkk-1), ANOVA with Tukey-Kramer multiple comparison test. (C): Histological evaluation of new bone formation after implantation. New bone formation in PBS, nAT-MSC, sAT-MSC, nAT-MSC + Mock, sAT-MSC + Mock, and sAT-MSC + shDkk-1 were evaluated histologically by hematoxylin and eosin staining. The arrows indicate the edges of host bone. Scale bar indicates 500 or 200 μm. (D): Immunohistochemistry analysis with anti-human osteopontin (hOPN) antibody was perfomed in PBS, nAT-MSC, sAT-MSC, nAT-MSC + Mock, sAT-MSC + Mock, and sAT-MSC + shDkk-1. The arrows indicate new bone expressing human osteopontin. Scale bar indicates 100 μm.

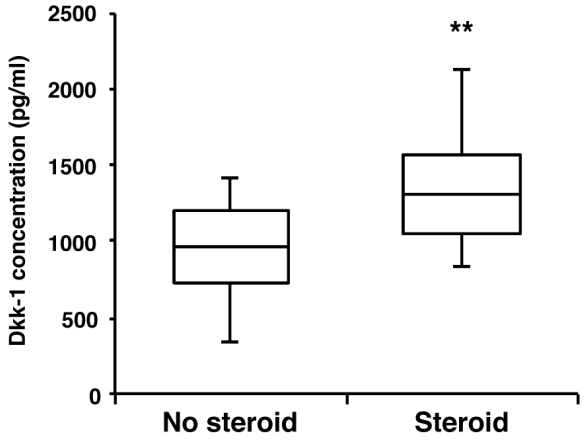

Figure 10. Measurement of plasma Dkk-1 level in steroid- and non-steroid-induced ONFH patients

Plasma Dkk-1 levels were determined by ELISA. No steroid: N=12, Steroid: N=17. **P < 0.01, Student's *t*-test.

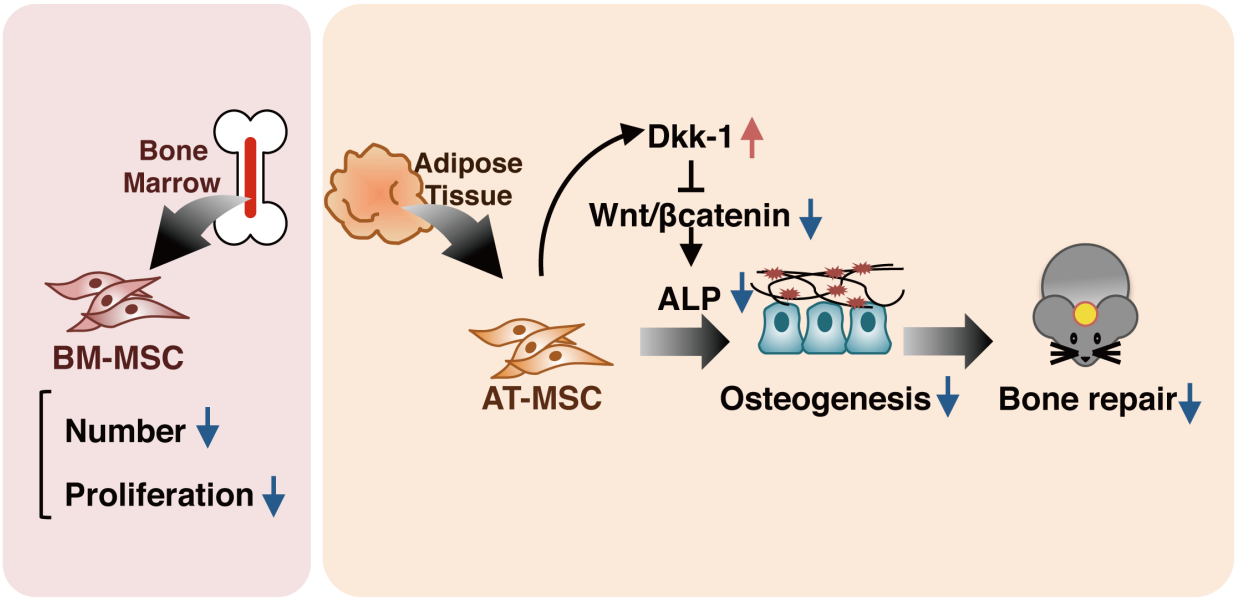

Figure 11. Study summary schematic in chapter 2

Glucocorticoid treatment reduces the number and the proliferative activity of BM-MSCs. The proliferative activity of AT-MSCs is not affected by glucocorticoid treatment, however, osteogenic ability is impaired by downregulation of ALP through Dkk-1/wnt/β-catenin signaling. The levels of Dkk-1 were not only upregulated in AT-MSCs but also in the plasma derived from steroid-induced ONFH patients.

Chapter III: Conclusion

In the present study, I demonstrated that chronic glucocorticoid treatment impaired the proliferative potential of BM-MSCs whereas proliferation in AT-MSCs derived from steroid-induced ONFH was not affected. On the other hand, the osteogenic ability of sAT-MSCs was impaired therough the downregukation of wnt/β-catenin signaling due to highly expressed Dkk-1. Interestingly, the elevated level of Dkk-1 was also observed in the plasma from steroid-induced ONFH patients (Fig. 11). These results suggest that BM-MSCs derived from steroid-induced ONFH are not useful because of their less and unstable proliferative ability. Although the proliferative ability of AT-MSCs was not impaired by glucocorticoid therapy, functional modification of sAT-MSCs would be required to obtain sufficient therapeutic effect. Dkk-1 would be a key factor to improve the bone regenerative function of sAT-MSC. In addition, Dkk-1 in plasma would be a diagnostic factor that reflects physiological condition of steroid-induced ONFH.

Reference

Barnes, P. J. (1998). Anti-inflammatory actions of glucocorticoids: molecular mechanisms. *Clinical science, 94*(6), 557-572.

Butler, J. S., Murray, D. W., Hurson, C. J., O'Brien, J., Doran, P. P., & O'Byrne, J. M. (2011). The role of Dkk1 in bone mass regulation: correlating serum Dkk1 expression with bone mineral density. *Journal of Orthopaedic Research, 29*(3), 414-418.

Cheng, S.-L., Yang, J. W., Rifas, L., Zhang, S.-F., & Avioli, L. V. (1994). Differentiation of human bone marrow osteogenic stromal cells in vitro: induction of the osteoblast phenotype by dexamethasone. *Endocrinology, 134*(1), 277-286.

Clevers, H. (2006). Wnt/β-catenin signaling in development and disease. *Cell, 127*(3), 469-480.

Cooper, M. S., & Hardy, R. (2011). Glucocorticoid-induced osteoporosis–a disorder of mesenchymal stromal cells? *Frontiers in endocrinology, 2*, 24.

Cowan, C. M., Shi, Y.-Y., Aalami, O. O., Chou, Y.-F., Mari, C., Thomas, R., . . . Longaker, M. T. (2004). Adipose-derived adult stromal cells heal critical-size mouse calvarial defects. *Nature biotechnology, 22*(5), 560-567.

Cox, G., Einhorn, T. A., Tzioupis, C., & Giannoudis, P. V. (2010). Bone-turnover markers in fracture healing. *J Bone Joint Surg Br, 92*(3), 329-334. doi:10.1302/0301-620x.92b3.22787

de Boer, J., Siddappa, R., Gaspar, C., van Apeldoorn, A., Fodde, R., & van Blitterswijk, C. (2004). Wnt signaling inhibits osteogenic differentiation of human mesenchymal stem cells. *Bone, 34*(5), 818-826.

Diarra, D., Stolina, M., Polzer, K., Zwerina, J., Ominsky, M. S., Dwyer, D., . . . Scheinecker, C. (2007). Dickkopf-1 is a master regulator of joint remodeling. *Nature medicine, 13*(2), 156-163.

Dominici, M., Le Blanc, K., Mueller, I., Slaper-Cortenbach, I., Marini, F., Krause, D., . . . Horwitz, E. (2006). Minimal criteria for defining multipotent mesenchymal stromal cells. The International Society for Cellular Therapy position statement. *Cytotherapy, 8*(4), 315-317.

Etheridge, S. L., Spencer, G. J., Heath, D. J., & Genever, P. G. (2004). Expression profiling and functional analysis of wnt signaling mechanisms in mesenchymal stem cells. *Stem Cells, 22*(5), 849-860.

Fedde, K. N., Blair, L., Silverstein, J., Coburn, S. P., Ryan, L. M., Weinstein, R. S., . . . Whyte, M. P. (1999). Alkaline phosphatase knock-out mice recapitulate the metabolic and skeletal defects of infantile hypophosphatasia. *J Bone Miner Res, 14*(12), 2015-2026. doi:10.1359/jbmr.1999.14.12.2015

FISHER, D. E., & BICKEL, W. H. (1971). Corticosteroid-induced avascular necrosis. *J Bone Joint Surg Am, 53*(5), 859-873.

Friedenstein, A. J., Chailakhjan, R. K., & Lalykina, K. S. (1970). The development of fibroblast colonies in monolayer cultures of guinea-pig

bone marrow and spleen cells. *Cell Tissue Kinet, 3*(4), 393-403.

Fukushima, W., Fujioka, M., Kubo, T., Tamakoshi, A., Nagai, M., & Hirota, Y. (2010). Nationwide epidemiologic survey of idiopathic osteonecrosis of the femoral head. *Clinical Orthopaedics and Related Research®, 468*(10), 2715-2724.

Gangji, V., De Maertelaer, V., & Hauzeur, J.-P. (2011). Autologous bone marrow cell implantation in the treatment of non-traumatic osteonecrosis of the femoral head: five year follow-up of a prospective controlled study. *Bone, 49*(5), 1005-1009.

Gaur, T., Lengner, C. J., Hovhannisyan, H., Bhat, R. A., Bodine, P. V., Komm, B. S., . . . Stein, G. S. (2005). Canonical WNT signaling promotes osteogenesis by directly stimulating Runx2 gene expression. *Journal of Biological Chemistry, 280*(39), 33132-33140.

Hayashi, K., Yamaguchi, T., Yano, S., Kanazawa, I., Yamauchi, M., Yamamoto, M., & Sugimoto, T. (2009). BMP/Wnt antagonists are upregulated by dexamethasone in osteoblasts and reversed by alendronate and PTH: potential therapeutic targets for glucocorticoid-induced osteoporosis. *Biochemical and biophysical research communications, 379*(2), 261-266.

Hernigou, P., & Beaujean, F. (2002). Treatment of osteonecrosis with autologous bone marrow grafting. *Clinical orthopaedics and related research, 405*, 14-23.

Hernigou, P., Beaujean, F., & Lambotte, J. (1999). Decrease in the

mesenchymal stem-cell pool in the proximal femur in corticosteroid-induced osteonecrosis. *Bone & Joint Journal, 81*(2), 349-355.

Hessle, L., Johnson, K. A., Anderson, H. C., Narisawa, S., Sali, A., Goding, J. W., . . . Millán, J. L. (2002). Tissue-nonspecific alkaline phosphatase and plasma cell membrane glycoprotein-1 are central antagonistic regulators of bone mineralization. *Proceedings of the National Academy of Sciences, 99*(14), 9445-9449.

Honsawek, S., Tanavalee, A., Yuktanandana, P., Ngarmukos, S., Saetan, N., & Tantavisut, S. (2010). Dickkopf-1 (Dkk-1) in plasma and synovial fluid is inversely correlated with radiographic severity of knee osteoarthritis patients. *BMC musculoskeletal disorders, 11*(1), 1.

Houdek, M. T., Wyles, C. C., Packard, B. D., Terzic, A., Behfar, A., & Sierra, R. J. (2016). Decreased Osteogenic Activity of Mesenchymal Stem Cells in Patients With Corticosteroid-Induced Osteonecrosis of the Femoral Head. *The Journal of Arthroplasty, 31*(4), 893-898.

Jones, L. C., & Hungerford, D. S. (2004). Osteonecrosis: etiology, diagnosis, and treatment. *Current opinion in rheumatology, 16*(4), 443-449.

Kajiyama, S., Ujiie, Y., Nishikawa, S., Inoue, K., Shirakawa, S., Hanada, N., . . . Gomi, K. (2015). Bone formation by human umbilical cord perivascular cells. *Journal of Biomedical Materials Research Part A, 103*(8), 2807-2814.

Khanh, V. C., Ohneda, K., Kato, T., Yamashita, T., Sato, F., Tachi, K., & Ohneda, O. (2017). Uremic Toxins Affect the Imbalance of Redox State and Overexpression of Prolyl Hydroxylase 2 in Human Adipose Tissue-Derived Mesenchymal Stem Cells Involved in Wound Healing. *Stem Cells Dev, 26*(13), 948-963. doi:10.1089/scd.2016.0326

Kimura, K., Nagano, M., Salazar, G., Yamashita, T., Tsuboi, I., Mishima, H., . . . Ohneda, O. (2013). The role of CCL5 in the ability of adipose tissue-derived mesenchymal stem cells to support repair of ischemic regions. *Stem cells and development, 23*(5), 488-501.

Ko, E., Alberti, K., Lee, J. S., Yang, K., Jin, Y., Shin, J., . . . Cho, S. W. (2016). Nanostructured Tendon-Derived Scaffolds for Enhanced Bone Regeneration by Human Adipose-Derived Stem Cells. *ACS Appl Mater Interfaces, 8*(35), 22819-22829. doi:10.1021/acsami.6b05358

Langenbach, F., & Handschel, J. (2013). Effects of dexamethasone, ascorbic acid and beta-glycerophosphate on the osteogenic differentiation of stem cells in vitro. *Stem Cell Res Ther, 4*(5), 117. doi:10.1186/scrt328

Lee, J. S., Lee, J. S., Roh, H. L., Kim, C. H., Jung, J. S., & Suh, K. T. (2006). Alterations in the differentiation ability of mesenchymal stem cells in patients with nontraumatic osteonecrosis of the femoral head: comparative analysis according to the risk factor. *Journal of Orthopaedic Research, 24*(4), 604-609.

Li, H., Dai, K., Tang, T., Zhang, X., Yan, M., & Lou, J. (2007). Bone regeneration

by implantation of adipose-derived stromal cells expressing BMP-2. *Biochem Biophys Res Commun, 356*(4), 836-842. doi:10.1016/j.bbrc.2007.02.165

Li, J., Sarosi, I., Cattley, R. C., Pretorius, J., Asuncion, F., Grisanti, M., . . . Qiu, W. (2006). Dkk1-mediated inhibition of Wnt signaling in bone results in osteopenia. *Bone, 39*(4), 754-766.

Lukert, B. P., & Raisz, L. G. (1990). Glucocorticoid-induced osteoporosis: pathogenesis and management. *Ann Intern Med, 112*(5), 352-364.

Marie, P. J. (2008). Transcription factors controlling osteoblastogenesis. *Archives of biochemistry and biophysics, 473*(2), 98-105.

Matsubara, T., Kida, K., Yamaguchi, A., Hata, K., Ichida, F., Meguro, H., . . . Yoneda, T. (2008). BMP2 regulates Osterix through Msx2 and Runx2 during osteoblast differentiation. *J Biol Chem, 283*(43), 29119-29125. doi:10.1074/jbc.M801774200

Mostafa, N. Z., Fitzsimmons, R., Major, P. W., Adesida, A., Jomha, N., Jiang, H., & Uludağ, H. (2012). Osteogenic differentiation of human mesenchymal stem cells cultured with dexamethasone, vitamin D3, basic fibroblast growth factor, and bone morphogenetic protein-2. *Connective tissue research, 53*(2), 117-131.

Mukhopadhyay, M., Sinha, R., Pal, M., Bhattacharyya, S., Dan, A., & Roy, M. M. (2011). Role of common biochemical markers for the assessment of fracture union. *Indian J Clin Biochem, 26*(3), 274-278.

doi:10.1007/s12291-011-0143-1

Muljacic, A., Poljak-Guberina, R., Zivkovic, O., Bilic, V., Guberina, M., & Crvenkovic, D. (2013). Course and rate of post-fracture bone healing in correlation with bone-specific alkaline phosphatase and bone callus formation. *Coll Antropol, 37*(4), 1275-1283.

Nagano, M., Kimura, K., Yamashita, T., Ohneda, K., Nozawa, D., Hamada, H., . . . Ohneda, O. (2010). Hypoxia responsive mesenchymal stem cells derived from human umbilical cord blood are effective for bone repair. *Stem cells and development, 19*(8), 1195-1210.

Ohnaka, K., Taniguchi, H., Kawate, H., Nawata, H., & Takayanagi, R. (2004). Glucocorticoid enhances the expression of dickkopf-1 in human osteoblasts: novel mechanism of glucocorticoid-induced osteoporosis. *Biochemical and biophysical research communications, 318*(1), 259-264.

Orimo, H. (2010). The mechanism of mineralization and the role of alkaline phosphatase in health and disease. *J Nippon Med Sch, 77*(1), 4-12.

Rawadi, G., Vayssière, B., Dunn, F., Baron, R., & Roman-Roman, S. (2003). BMP-2 controls alkaline phosphatase expression and osteoblast mineralization by a Wnt autocrine loop. *Journal of Bone and Mineral Research, 18*(10), 1842-1853.

Rhen, T., & Cidlowski, J. A. (2005). Antiinflammatory action of glucocorticoids--new mechanisms for old drugs. *N Engl J Med, 353*(16), 1711-1723. doi:10.1056/NEJMra050541

Salazar, V. S., Gamer, L. W., & Rosen, V. (2016). BMP signalling in skeletal development, disease and repair. *Nat Rev Endocrinol, 12*(4), 203-221. doi:10.1038/nrendo.2016.12

Sanderson, M., Sadie-Van Gijsen, H., Hough, S., & Ferris, W. F. (2015). The Role of MKP-1 in the Anti-Proliferative Effects of Glucocorticoids in Primary Rat Pre-Osteoblasts. *PLoS One, 10*(8), e0135358. doi:10.1371/journal.pone.0135358

Sato, K., Itoh, T., Kato, T., Kitamura, Y., Kaul, S. C., Wadhwa, R., . . . Ohneda, O. (2015). Serum-free isolation and culture system to enhance the proliferation and bone regeneration of adipose tissue-derived mesenchymal stem cells. *In Vitro Cellular & Developmental Biology-Animal, 51*(5), 515-529.

Schäcke, H., Döcke, W.-D., & Asadullah, K. (2002). Mechanisms involved in the side effects of glucocorticoids. *Pharmacology & therapeutics, 96*(1), 23-43.

Schleimer, R. (1993). An overview of glucocorticoid anti-inflammatory actions. *European journal of clinical pharmacology, 45*(1), S3-S7.

Sen, R. K., Tripathy, S. K., Aggarwal, S., Marwaha, N., Sharma, R. R., & Khandelwal, N. (2012). Early results of core decompression and autologous bone marrow mononuclear cells instillation in femoral head osteonecrosis: a randomized control study. *The Journal of Arthroplasty, 27*(5), 679-686.

Serena, C., Keiran, N., Ceperuelo-Mallafre, V., Ejarque, M., Fradera, R., Roche, K., . . . Fernandez-Veledo, S. (2016). Obesity and Type 2 Diabetes Alters the Immune Properties of Human Adipose Derived Stem Cells. *Stem Cells, 34*(10), 2559-2573. doi:10.1002/stem.2429

Shao, X., Lin, S., Peng, Q., Shi, S., Wei, X., Zhang, T., & Lin, Y. (2017). Tetrahedral DNA Nanostructure: A Potential Promoter for Cartilage Tissue Regeneration via Regulating Chondrocyte Phenotype and Proliferation. *Small, 13*(12). doi:10.1002/smll.201602770

Shao, X. R., Lin, S. Y., Peng, Q., Shi, S. R., Li, X. L., Zhang, T., & Lin, Y. F. (2017). Effect of tetrahedral DNA nanostructures on osteogenic differentiation of mesenchymal stem cells via activation of the Wnt/beta-catenin signaling pathway. *Nanomedicine, 13*(5), 1809-1819. doi:10.1016/j.nano.2017.02.011

Stucki, U., Schmid, J., Hammerle, C. F., & Lang, N. P. (2001). Temporal and local appearance of alkaline phosphatase activity in early stages of guided bone regeneration. A descriptive histochemical study in humans. *Clin Oral Implants Res, 12*(2), 121-127.

Suzuki, A., Palmer, G., Bonjour, J.-P., & Caverzasio, J. (1999). Regulation of Alkaline Phosphatase Activity by p38 MAP Kinase in Response to Activation of Gi Protein-Coupled Receptors by Epinephrine in Osteoblast-Like Cells 1. *Endocrinology, 140*(7), 3177-3182.

Tian, E., Zhan, F., Walker, R., Rasmussen, E., Ma, Y., Barlogie, B., &

Shaughnessy Jr, J. D. (2003). The role of the Wnt-signaling antagonist DKK1 in the development of osteolytic lesions in multiple myeloma. *New England Journal of Medicine, 349*(26), 2483-2494.

Tran, T. C., Kimura, K., Nagano, M., Yamashita, T., Ohneda, K., Sugimori, H., . . . Yoshikawa, H. (2011). Identification of human placenta-derived mesenchymal stem cells involved in re-endothelialization. *Journal of cellular physiology, 226*(1), 224-235.

Trinh, N.-T., Yamashita, T., Ohneda, K., Kimura, K., Salazar, G. T. a., Sato, F., & Ohneda, O. (2016). Increased expression of EGR-1 in diabetic human adipose tissue-derived mesenchymal stem cells reduces their wound healing capacity. *Stem cells and development, 25*(10), 760-773.

Tsuji, K., Bandyopadhyay, A., Harfe, B. D., Cox, K., Kakar, S., Gerstenfeld, L., . . . Rosen, V. (2006). BMP2 activity, although dispensable for bone formation, is required for the initiation of fracture healing. *Nat Genet, 38*(12), 1424-1429. doi:10.1038/ng1916

Uccelli, A., Moretta, L., & Pistoia, V. (2008). Mesenchymal stem cells in health and disease. *Nat Rev Immunol, 8*(9), 726-736. doi:10.1038/nri2395

Urbaniak, J. R., Coogan, P. G., Gunneson, E. B., & Nunley, J. A. (1995). Treatment of osteonecrosis of the femoral head with free vascularized fibular grafting. A long-term follow-up study of one hundred and three hips. *The Journal of Bone & Joint Surgery, 77*(5), 681-694.

Wang, B. L., Sun, W., Shi, Z. C., Lou, J. N., Zhang, N. F., Shi, S. H., . . . Zhang,

W. J. (2008). Decreased proliferation of mesenchymal stem cells in corticosteroid-induced osteonecrosis of femoral head. *Orthopedics, 31*(5).

Weinstein, R. S. (2012). Glucocorticoid-induced osteonecrosis. *Endocrine, 41*(2), 183-190.

Wennberg, C., Hessle, L., Lundberg, P., Mauro, S., Narisawa, S., Lerner, U. H., & Millan, J. L. (2000). Functional characterization of osteoblasts and osteoclasts from alkaline phosphatase knockout mice. *J Bone Miner Res, 15*(10), 1879-1888. doi:10.1359/jbmr.2000.15.10.1879

Wu, L. A., Wang, F., Donly, K. J., Baker, A., Wan, C., Luo, D., . . . Chen, S. (2016). Establishment of Immortalized BMP2/4 Double Knock-Out Osteoblastic Cells Is Essential for Study of Osteoblast Growth, Differentiation, and Osteogenesis. *J Cell Physiol, 231*(6), 1189-1198. doi:10.1002/jcp.25266

Wyles, C. C., Houdek, M. T., Crespo-Diaz, R. J., Norambuena, G. A., Stalboerger, P. G., Terzic, A., . . . Sierra, R. J. (2015). Adipose-derived mesenchymal stem cells are phenotypically superior for regeneration in the setting of osteonecrosis of the femoral head. *Clinical Orthopaedics and Related Research®, 473*(10), 3080-3090.

Xie, Q., Wang, Z., Zhou, H., Yu, Z., Huang, Y., Sun, H., . . . Fan, X. (2016). The role of miR-135-modified adipose-derived mesenchymal stem cells in bone regeneration. *Biomaterials, 75*, 279-294. doi:10.1016/j.biomaterials.2015.10.042

Yamanaka, S., Yokote, S., Yamada, A., Katsuoka, Y., Izuhara, L., Shimada, Y., . . . Yokoo, T. (2014). Adipose tissue-derived mesenchymal stem cells in long-term dialysis patients display downregulation of PCAF expression and poor angiogenesis activation. *PLoS One, 9*(7), e102311. doi:10.1371/journal.pone.0102311

Yao, W., Cheng, Z., Busse, C., Pham, A., Nakamura, M. C., & Lane, N. E. (2008). Glucocorticoid excess in mice results in early activation of osteoclastogenesis and adipogenesis and prolonged suppression of osteogenesis: a longitudinal study of gene expression in bone tissue from glucocorticoid-treated mice. *Arthritis & Rheumatism, 58*(6), 1674-1686.

Yao, W., Cheng, Z., Pham, A., Busse, C., Zimmermann, E. A., Ritchie, R. O., & Lane, N. E. (2008). Glucocorticoid-induced bone loss in mice can be reversed by the actions of parathyroid hormone and risedronate on different pathways for bone formation and mineralization. *Arthritis & Rheumatism, 58*(11), 3485-3497.

Yoshioka, T., Mishima, H., Akaogi, H., Sakai, S., Li, M., & Ochiai, N. (2011). Concentrated autologous bone marrow aspirate transplantation treatment for corticosteroid-induced osteonecrosis of the femoral head in systemic lupus erythematosus. *International orthopaedics, 35*(6), 823-829.

Acknowledgement

I sincerely express the deepest appreciation to Prof. Osamu Ohneda, the Department of Regenerative Medicine and Stem Cell Biology, University of Tsukuba, for the kind support during my doctoral course. I appreciate the time and patience you gave me. From the beginning time of my study till now, you have been given me much valuable advice and motivation in doing research.

In addition, I would like to appreciate Dr. Mami Matsuo-Takasaki, Dr. Toshiharu Yamashita, and Dr. Masumi Nagano, the Department of Regenerative Medicine and Stem Cell Biology, University of Tsukuba, for their kind guidance and discussion.

To fulfill this dissertation, I would like to thank the thesis committee members, Dr. Akiyoshi Fukamizu, Dr. Bernd K. Fleischmann, Dr. Yukihiro Yada, Dr. Hiroyuki Suzuki for the kind comments and the important advice.

I would like to express my gratitude to Dr. Hajime Mishima, Dr. Tomokazu Yoshioka, and Dr. Hisashi Sugaya, the Department of Orthopedic Surgery, University of Tsukuba, for your insightful discussion and providing the bone marrow, adipose tissue and plasma sample for this study.

I greatly appreciate to all members in Prof. Ohneda's Laboratory for your friendship and kind supports. Especially, I am grateful to Dr. Kazutoshi Sato and Dr. Vuong Cat Khanh for your kind help and discussion.

In addition, I would like to appreciate to the faculties in Ph. D. Program

in Human Biology (HBP) and the officers in the School of Integrative and Global Majors (SIGMA).

Finally, I would like to appreciate my family and friends for all the help and support.